EBioMedicine 61 (2020) 103061

Contents lists available at ScienceDirect

EBioMedicine

journal homepage: www.elsevier.com/locate/ebiom

Research paper

SP6616 as a Kv2.1 inhibitor efficiently ameliorates peripheral neuropathy in diabetic mice

Xialin Zhu[a,1], Yun Chen[b,1], Xu Xu[a,1], Xiaoju Xu[a], Yin Lu[a], Xi Huang[a], Jinpei Zhou[b], Lihong Hu[a], Jiaying Wang[a], Xu Shen[a,*]

[a] Jiangsu Key Laboratory for Pharmacology and Safety Evaluation of Chinese Materia Medica, Nanjing University of Chinese Medicine, Nanjing 210023, China
[b] Department of Medicinal Chemistry, China Pharmaceutical University, 24 Tongjia Xiang, Nanjing 210009, China

ARTICLE INFO

Article History:
Received 12 March 2020
Revised 20 September 2020
Accepted 24 September 2020
Available online xxx

Keywords:
SP6616
Kv2.1
Diabetic peripheral neuropathy
Dorsal root ganglion
Diabetes

ABSTRACT

Background: Diabetic peripheral neuropathy (DPN) is a common complication of diabetes severely afflicting the patients, while there is yet no effective medication against this disease. As Kv2.1 channel functions potently in regulating neurological disorders, the present work was to investigate the regulation of Kv2.1 channel against DPN-like pathology of DPN model mice by using selective Kv2.1 inhibitor SP6616 (ethyl 5-(3-ethoxy-4-methoxyphenyl)-2-(4-hydroxy-3-methoxybenzylidene)-7-methyl-3-oxo-2,3-dihydro-5H-[1,3]thiazolo[3,2-a]pyrimidine-6-carboxylate) as a probe.

Methods: STZ-induced type 1 diabetic mice with DPN (STZ mice) were defined at 12 weeks of age (4 weeks after STZ injection) through behavioral tests, and *db/db* (BKS Cg-$m^{+/+}Lepr^{db}$/J) type 2 diabetic mice with DPN (*db/db* mice) were at 18 weeks of age. SP6616 was administered daily via intraperitoneal injection for 4 weeks. The mechanisms underlying the amelioration of SP6616 on DPN-like pathology were investigated by RT-PCR, western blot and immunohistochemistry technical approaches against diabetic mice, and verified against the STZ mice with Kv2.1 knockdown in dorsal root ganglion (DRG) tissue by injection of adeno associated virus AAV9-Kv2.1-RNAi. Amelioration of SP6616 on the pathological behaviors of diabetic mice was assessed against tactile allodynia, thermal sensitivity and motor nerve conduction velocity (MNCV).

Findings: SP6616 treatment effectively ameliorated the threshold of mechanical stimuli, thermal sensitivity and MNCV of diabetic mice. Mechanism research results indicated that SP6616 suppressed Kv2.1 expression, increased the number of intraepidermal nerve fibers (IENFs), improved peripheral nerve structure and vascular function in DRG tissue. In addition, SP6616 improved mitochondrial dysfunction through Kv2.1/CaMKKβ/AMPK/PGC-1α pathway, repressed inflammatory response by inhibiting Kv2.1/NF-κB signaling and alleviated apoptosis of DRG neuron through Kv2.1-mediated regulation of Bcl-2 family proteins and Caspase-3 in diabetic mice.

Interpretation: Our work has highly supported the beneficial of Kv2.1 inhibition in ameliorating DPN-like pathology and highlighted the potential of SP6616 in the treatment of DPN.

Funding: Please see funding sources.

1. Introduction

Diabetic peripheral neuropathy (DPN) is a common complication of diabetes affecting more than two-thirds of diabetic patients [1, 2]. Clinical features of DPN include a series of peripheral nerve structural changes such as axonal degeneration, intraepithelial nerve fiber loss, segmental demyelination and microangiopathy [3–6]. DPN pathogenesis is very complicated involving multiple risk factors, including oxidative stress, mitochondrial dysfunction, neuroinflammation and neuronal apoptosis [7, 8]. Unfortunately, the current clinic treatments are lack of specificity and hard to achieve the desired therapeutic effects [9]. Thus, it is imperative to design efficient medications against DPN based on new therapeutic strategies and targets.

Voltage gated potassium (Kv) channel is tightly implicated in varied physiological functions of cells such as neuronal discharge pattern regulation, synaptic integration, action potential shape and neurotransmitter release [10]. Abnormal structure or dysfunction of Kv channel can cause various diseases, like neurodegenerative [11] and metabolic diseases [12]. Kv channel is classified by 12 subfamilies, and Kv2 channel family mainly has two members Kv2.1 and Kv2.2. In

* Corresponding author.
E-mail addresses: zhjp@cpu.edu.cn (J. Zhou), wangjy@njucm.edu.cn (J. Wang), xshen@njucm.edu.cn (X. Shen).
[1] These authors contributed equally to this work.

https://doi.org/10.1016/j.ebiom.2020.103061

Research in context

Evidence before this study

DPN is highly accompanied with abnormal sensory disorders and peripheral nerve structural changes, and its pathogenesis is tightly related to mitochondrial dysfunction, inflammation and apoptosis. Kv2.1 channel is expressed in dorsal root ganglion (DRG) neuron and participates in the regulation of sensory neuron excitability, afferent myelin and neurological disorders. It is thus suggested that Kv2.1 channel should function potently in the regulation of DPN pathology and Kv2.1 inhibition may exhibit beneficial in DPN treatment.

Added value of this study

We reported that small molecular compound SP6616 as an inhibitor of Kv2.1 channel efficiently ameliorated DPN-like pathology in both STZ-induced type 1 (STZ) and *db/db* type 2 diabetic (*db/db*) mice. The underlying mechanisms have been intensively investigated by assay against STZ mice with Kv2.1 knockdown in DRG tissue injected with adeno associated virus AAV9-Kv2.1-RNAi. SP6616 treatment promoted neurite growth of DRG neuron by inhibiting Kv2.1 channel, improved mitochondrial dysfunction through Kv2.1/CaMKKβ/AMPK/PGC-1α pathway, suppressed inflammation by inhibiting Kv2.1/NF-κB signaling and alleviated apoptosis of DRG neuron through Kv2.1-mediated regulation against Bcl-2 family proteins and Caspase-3 in diabetic mice.

Implications of all the available evidence

There is currently lack of effective target or strategy for drug design against DPN. Our findings have provided new evidence that Kv2.1 inhibition may function potently in the amelioration of DPN pathology and highlighted the potential of SP6616 as a Kv2.1 inhibitor in the treatment of this disease.

structure, Kv2.1 is composed by four α subunits, four potassium selective channels and β subunits. Kv2.1 as a major member of Kv2 family possesses 65-80% of the total Kv currents.

Kv2.1 channel is highly expressed in rodent dorsal root ganglion (DRG) neuron and implicated in the regulation of sensory neuron excitability, afferent myelin and neurological disorders including neuropathic pain and epilepsy [13, 14]. In late period, clinical manifestation of DPN is characterized by loss of sensation and hypoalgesia. Kv2.1 dysfunction exists in chronic pain conditions [15]. Demyelination of DRG neuron is one of the most obviously pathological features of DPN and damaged myelin blocks the conduction of action potential on axons [16, 17], while blockage of Kv channel has been reported to improve axonal conduction [18]. Notably, AMPK/PGC-1α signaling plays a potent role in the regulation of mitochondrial function that is tightly involved in energy metabolism of DPN [19, 20], and AMPK activation relies on the phosphorylation of the upstream protein CaMKKβ [21], which is regulated by Kv2.1 channel through intracellular Ca^{2+} flux [22]. As such, Kv2.1 channel was believed to function in the regulation of mitochondria-related events [23]. Moreover, Kv2.1 inhibitor was reported to repress inflammation and apoptosis that are tightly involved in DPN pathogenesis [24, 25]. Therefore, all the facts have strongly suggested the potential involvement of Kv2.1 regulation in DPN pathology.

In the current work, we determined that our previously reported Kv2.1 inhibitor SP6616 (5-(3-ethoxy-4-methoxyphenyl)-2-(4-hydroxy-3-methoxybenzylidene)-7-methyl-3-oxo-2,3-dihydro-5H [1,3] thiazolo [3,2-a] pyrimidine-6-carboxylate (Fig. 1a) [26] efficiently ameliorated peripheral neuropathy in diabetic mice. The underlying mechanisms have been investigated by assay against the diabetic mice with *in vivo* Kv2.1 knockdown in DRG tissue by injection of adeno associated virus AAV9-Kv2.1-RNAi. Our work has supported that inhibition of Kv2.1 channel might be a promising strategy for drug discovery against DPN and highlighted the potential of SP6616 in the treatment of this disease.

2. Materials and methods

2.1. DRG neuron cultured from adult mice

DRG neuron from adult mice was cultured by the published approach [27]. Briefly, DRG neuron was isolated from normal or diabetic mice, and plated onto poly-d-L-ornithine hydrobromide and laminin coated 12-well glass slides or 96-well plates. The neuron was cultured in Hams F-12 medium (Gibco) with N2 supplement (Thermo Fisher) or B27 (Thermo Fisher), 0.1 ng/ml nerve growth factor (Sigma-Aldrich), 100 U/ml penicillin and 100 mg/ml streptomycin (PS). In all the studies, neuron from age-matched control mice was cultured with 10 nM insulin and 10 mM D-glucose, and neuron from diabetic mice was cultured with 25 mM D-glucose without insulin.

2.2. Total neurite outgrowth determination

Total neurite outgrowth was determined according to the published procedure [3, 28]. Briefly, DRG neuron extracted from mice was plated into cell slides overnight, followed by incubation with 4% polyformaldehyde for 15 min at room temperature. Then, it was permeabilized with 0.3% Triton X-100 for 5 min and washed 3 times by PBS (pH7.4). After incubated with 3% goat serum for 1h, DRG neuron was treated with primary antibody β-tubulin isotype Ⅲ (1:1000; Sigma-Aldrich) overnight at 4°C, followed by incubation with secondary antibody Alexia Fluor 488 goat anti-Mouse IgG(H+L) (Proteintech) for 1h at room temperature. The fluorescent images were collected by fluorescent microscope (Leica, Germany). The total length of neurite outgrowth was quantified by Neuron J plug-in components in ImageJ software.

2.3. MTT assay

DRG neuron was isolated from normal mice (C57BL/6J) and plated into 96-well plates, followed by incubation with SP6616 (2, 10μM) for 24 h. MTT was added into 96-well plates (final concentration 500 μg/ml) and incubated with the cells for 2h at 37°C. Then, the plates were added by 100 μl of dimethyl sulfoxide (DMSO: Sigma-Aldrich) and shook 15 min at room temperature. The absorbance of the cells was detected at 490 nm.

2.4. Mitochondrial function assessment

Mitochondrial respiration was evaluated by an XF96 Analyzer (Seahorse Biosciences). In the assay, DRG neuron from mice was seeded and cultured with Hams F-12 medium (Gibco) in specialized 96-well microplates for monitoring oxygen consumption rate (OCR) in real time. One hour before the assay, the culture medium (Hams F-12 medium) was changed to basal medium (unbuffered Dulbecco's modified Eagle's medium (pH 7.4)) supplemented with 1 mM pyruvate (Gibco), 2 mM L-glutamine and 10 mM D-glucose. In the assay, oligomycin (1 μM), carbonyl cyanide4-(trifluoromethoxy) phenylhydrazone (FCCP, 1 μM) and a combination of rotenone (1 μM) with antimycin A (1 μM) were injected sequentially through ports in the Seahorse Flux Pak cartridges to measure the oxygen consumption rate (OCR), basal respiration, maximal respiration, ATP production and spare respiratory capacity of DRG neuron.

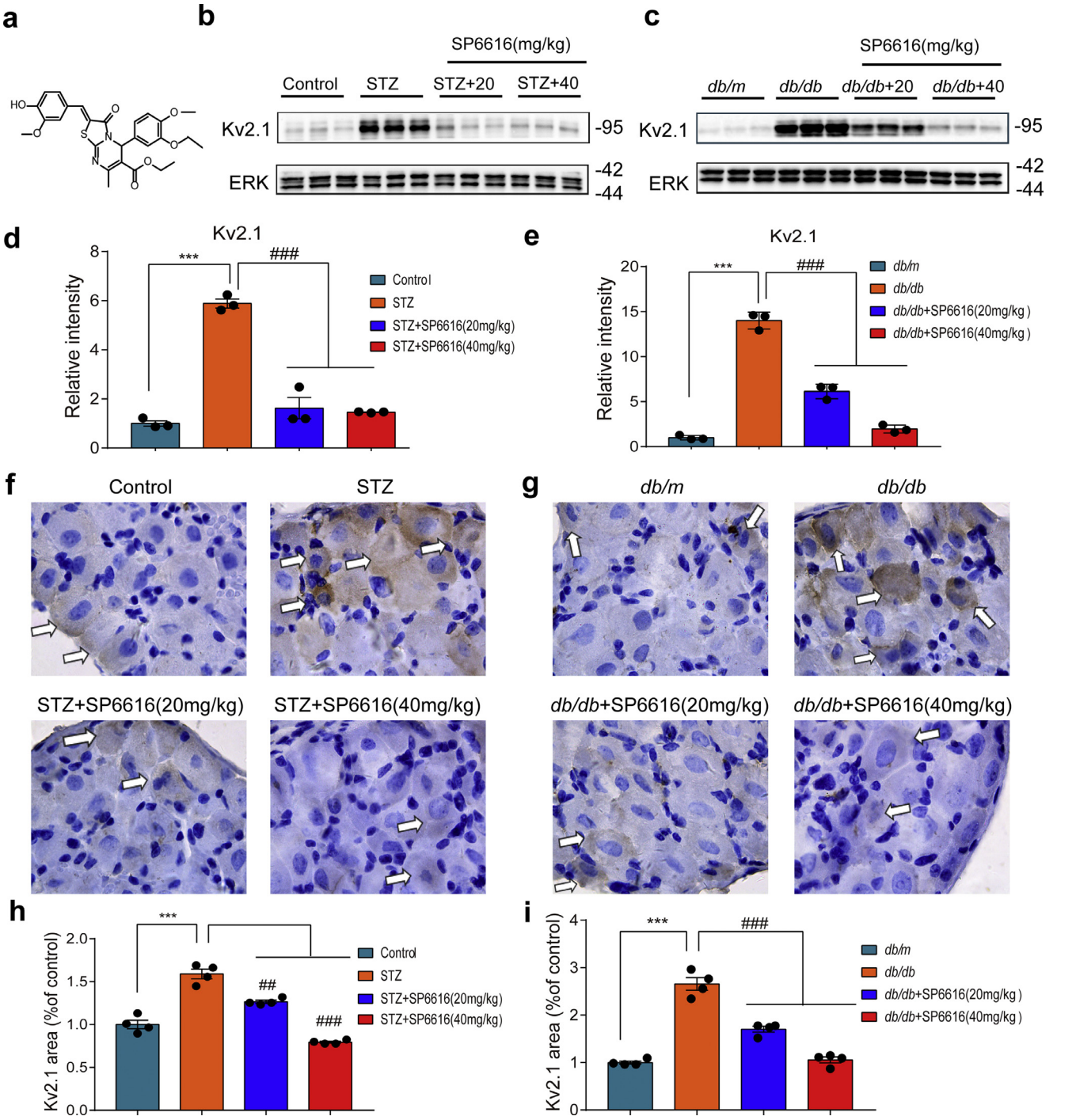

Fig. 1. SP6616 treatment suppressed Kv2.1 expression in DRG tissue of diabetic mice(**a**) Structure of SP6616. [26] (**b, c**) Representative immuno-fluorescent images showing Kv2.1 expression in DRG tissue from age-matched non-diabetic mice (Control, age-matched C57BL/6 mice as control in the related assay for STZ-induced type 1 diabetic mice with DPN; *db/m*, age-matched heterozygotes mice with nonpenetrant genotype as control in the related assay for *db/db* type 2 diabetic mice with DPN. The same hereinafter.), diabetic mice (STZ, type 1 diabetic mice with DPN; *db/db*, type 2 diabetic mice with DPN) and SP6616 (20, 40 mg/kg)-treated diabetic mice (STZ + 20, 40 mg/kg; *db/db* + 20, 40 mg/kg) (n = 3). (**d, e**) Quantification for (**b, c**). (**f, g**) Immunohistochemical results showing Kv2.1 expression in DRG tissue from control mice (Control, *db/m*), diabetic mice (STZ, *db/db*) and SP6616 (20, 40 mg/kg)-treated diabetic mice (STZ + 20, 40 mg/kg; *db/db* + 20, 40 mg/kg) (n = 4). (**h, i**) Quantification for (**f, g**). All the expressions were normalized to total extracellular regulated protein kinase (T-ERK) level. All the values were presented as mean ± SEM. $^{***}P < 0.001$ *vs* Control or *db/m* (Student's t-test); $^{##}P < 0.01$, $^{###}P < 0.001$ *vs* STZ or *db/db* (one-way ANOVA with Dunnett's post-hoc test).

2.5. Mitochondrial membrane potential detection

DRG neuron from the mice was plated into 96-well plates for detecting mitochondrial membrane potential (MMP) according to the experimental instructions by JC-1 staining solution. Ratio of fluorescence (530/590) was detected by fluorescent microplate reader.

2.6. Real-time intracellular Ca^{2+} assay

DRG neuron from 8-week old C57BL/6J mice was seeded into 96-well glass plates overnight, and Fluo-4 AM (final concentration 4 μM) working solution was then added to the cells and incubated at 37°C for 40 min, followed by incubation with HBSS at 37°C for 20-30 min.

By considering that SP6616 (2, 10 μM) rendered no effects on cell viability in DRG neuron by MTT assay (Fig. S1a) but exhibited activity in increasing intracellular Ca^{2+} level [26], we thus selected SP6616 at 10 μM to detect Ca^{2+} influx in DRG neuron and at 2 and 10 μM to verify its dose-dependent effect. Finally, SP6616 (2, 10 μM) or nifedipine (20 μM) was added into the wells and assayed by FlexStation3 (USA). Data were shown by the area under the original curve (AUC).

2.7. Quantitative real-time PCR assay

Total mRNA in DRG tissue was extracted by TRIzol reagent (TaKaRa Biotechnology Co). Reverse-PCR kit (TaKaRa Biotechnology Co) was used to gather cDNA. RT-PCR assay was performed by SYBR green PCR core reagent kit (TaKaRa Biotechnology Co).

PCR primer sequences were performed as follows. Kv2.1: forward, TCGACAACACGTGCTGTGCT; reverse, GGCCAACTTCAGGATGCGC, mouse. β-actin: forward, TCATCACTATTGGCAACGAGC; reverse, AACAGTCCGCCTAGAAGCAC, mouse.

2.8. Immunohistochemistry assay

The foot pad or DRG tissue of mice was made into paraffin blocks by paraffin-embedded immunohistochemistry assay (IHC-P). Paraffin blocks were cut into 6 μm-thick sections and stained with PGP9.5 antibody or Kv2.1 antibody (diluted by 3% goat serum and 0.5% Triton X-100 for 1: 1,000) overnight. Sections were incubated with DAB (Zsbio) for 5 min, and images were collected by fluorescence microscope (Leica, Germany). Number of fiber or area of Kv2.1 protein distribution was quantified by Image J software. Antibodies for immunohistochemistry assay were provided in Supplementary Table 1.

2.9. Western blot and enzyme-linked immunosorbent assay

DRG tissue from mice was lysed with RIPA buffer (Beyotime) including protease and phosphatase inhibitor cocktails (Thermo Scientific). Different proteins were separated by SDS-PAGE, transferred into nitrocellulose membrane (GE Healthcare, USA) and incubated with skimmed milk for over 30 min. Then, primary antibodies were incubated with nitrocellulose membrane at 4 °C overnight, followed by incubation with secondary antibodies for 2h at room temperature. The targeted protein bands were detected by Western ECL Substrate (Bio-Rad, USA). Total extracellular regulated protein kinase (T-ERK) was used as loading control instead of GAPDH due to the better stability of T-ERK in DRG tissue [3, 20, 27], and DRG tissue was pooled by large neuron, middle neuron and small neuron. Antibodies for western blot were provided in Supplementary Table 2.

Enzyme-linked immunosorbent assay (ELISA) was carried out by commercial kits (Nanjing Jiancheng Bioengineering Institute) to detect the levels of inflammatory cytokines TNF-α, IL-1β and IL-6, hormone levels of adrenocorticotropic hormone (ACTH) and corticosterone (CORT), cardiac lesion indexes cardiac troponin-T (cTn-T) and cardiac troponin-I (cTn-I) in the serum of mice. Insulin level in the serum of diabetic mice was detected by insulin commercial kit (Merck) and read by absorbance at 450 and 590 nm.

2.10. Biochemical index assessment

Levels of creatinine and urea nitrogen in the serum of diabetic mice were detected by commercial kits (Nanjing Jiancheng Bioengineering Institute). ALT and AST levels were evaluated by biochemical analyses (Model AU-480; Beckman Coulter, Fullerton, CA, USA).

2.11. Tactile allodynia and thermal sensitivity determination

Tactile allodynia determination- Von Frey filaments (Ugo Basile, Comerio VA, Italy) were used to measure tactile allodynia on hind paw of mice as previously described [29]. Briefly, the mice stood on a metal grid with hind paw full contact with Von Frey filaments. Mice were provided 15 min to suit surroundings before testing. Then hind paws were detected by diffident Von Frey filaments, and each Von Frey filament was held for 6-8s to confirm the stimulus response. Distribution of the sciatic nerve in mid-plantar left hind paw area was tested. A 50% paw withdrawal threshold was calculated according to the recorded values and analyzed by GraphPad Prism7.

Thermal sensitivity determination- Thermal sensitivity of mice was determined by thermal testing apparatus (Ugo Basile, Comerio VA, Italy) as previously described [30]. Briefly, mice were placed on the platform of thermal testing apparatus (Ugo Basile, Comerio VA, Italy) and adapted to warmed glass surface at least 15 min. The paw withdrawal latency was recorded from the onset of the irradiation (lamp 40 W, distance lamp to paw 40 mm) to the withdrawal of the hind paw at 25°C. The paw withdrawal latency data were calculated three times, and average withdrawal time was used for statistical analysis. The minimum interval of each set of the hind paw was five min.

2.12. Electrophysiology test

Motor nerve conduction velocity was evaluated by the previously published approaches [31, 32]. Briefly, mice were placed on a heated pad in a room maintained at 25°C to ensure a constant rectal temperature at 37°C. The motor nerve conduction velocity (MNCV) of the sciatic nerve ranging from ankle to sciatic notch was measured via bipolar electrodes with a supramaximal stimulus (3V) of 0.05 ms duration.

2.13. Regional blood flow velocity and perfused blood vessel area assessments

Mice were anesthetized with isoflurane (anesthesia machine, RWD, China), and the real-time regional blood flow velocity and perfused blood vessel area in foot pad and sciatic nerve were detected by Laser Speckle Contrast Imaging/LSCI (RFLSI Pro, RWD, China).

2.14. Ethics statement

All the animals were maintained in compliance with the Regulations for the Administration of Affairs Concerning Experimental Animals made by the Ministry of Science and Technology of China. All the animal-related experiments followed the institutional ethical guidelines on animal care of Nanjing University of Chinese Medicine (ethics number: 201901A005).

2.15. Animals

All the animals were received humane care and raised in 12h light-dark cycle barrier with temperature maintained around 20-25° C. Animals were full access to sterilized food and fresh water.

Male C57BL/6J mice at 7-week age were purchased from Vital River Laboratory Animal Technology Co (Beijing, China), and male BKS Cg-$m^{+/+}Lepr^{db}$/J (*db/db*) mice at 17-week age were purchased from Model Animal Research Center of Nanjing University.

Type 1 diabetic mice with DPN- Type 1 diabetic mice with DPN were obtained by the published approach [33]. Briefly, STZ (Sigma Aldrich, 150 mg/kg) was injected once to 8-week old male C57BL/6J mice. Type 1 diabetic mice were defined as a blood glucose level more than 16 mmol/L (~288 mg/dl) [34] and type 1 diabetic mice with DPN (STZ) were defined at 12 weeks of age (4 weeks after STZ injection) through behavioral tests. Age-matched C57BL/6J mice were used as control (Control) in STZ mice related assay.

Type2 diabetic mice with DPN- According to the literature method [35], *db/db* mice aged 18 weeks could be treated as type 2 diabetic mice with DPN (*db/db*). Age-matched heterozygotes mice with

nonpenetrant genotype were used as control (*db/m*) in *db/db* mice related assay. *db/db* mice belong to the highly inbred strains with a recessive autosomal mutation locus on chromosome 4 [36] and fail to respond to leptin receptor and produce hyperglycemia and hyperinsulinemia at 5-week age.

Kv2.1 knockdown in DRG tissue of STZ mice by injection of AAV9-Kv2.1-RNAi- Specific Kv2.1 siRNA sequence (CAGAGTCTGACAGAACTCCTA) was purchased from QIAGEN. Adeno associated virus AAV9-Kv2.1-RNAi and negative control vector (AAV9-NC) were purchased from Shanghai Genechem Co., Ltd. After treatment of STZ for four weeks, STZ mice were injected with AAV9-Kv2.1-RNAi (n = 36) or AAV9-NC (n = 12) at a titer of 1.0×10^{11} vector genomes/ml intravenously. After injection of AAV9-Kv2.1-RNAi or AAV9-NC for two weeks, Kv2.1 expression in DRG tissue from mice was detected by RT-PCR and western blot assays. The results demonstrated that the level of Kv2.1 expression was decreased by 40% with AAV9-Kv2.1-RNAi treatment (Fig. S2a-c; N = 3). Based on the published reports, $Kv2.1^{-/-}$ mice exhibited low level of fasting blood glucose [37, 38] and 40-60% knockdown rate of related target protein was acceptable for *in vivo* assays [39–41]. Thus, a 40% knockdown rate of Kv2.1 expression in DRG tissue from the STZ mice treated with AAV9-Kv2.1-RNAi was set up in the current work, and this kind of Kv2.1 knockdown DPN model mice was applied to use.

Additionally, we also investigated Kv2.2 level in mice. As indicated in Fig. S2d-e, no significant difference was found for Kv2.2 expression in DRG tissue between AAV9-Kv2.1-RNAi injected STZ mice (STZ+AAV9-Kv2.1-RNAi) (n = 3) and AAV9-NC injected STZ mice (STZ+ AAV9-NC) (n = 3).

All the results thus determined the specific Kv2.1 knockdown in DRG tissue of STZ mice by injection of AAV9-Kv2.1-RNAi.

2.16. Animal administration

SP6616 was dissolved in physiological saline with 2% DMSO (Sigma-Aldrich) and 8% Tween-80 (Sigma-Aldrich). In all the experiments, Control, diabetic mice (STZ, *db/db)* and AAV9-Kv2.1-RNAi injected STZ mice were daily administrated with SP6616 (20, 40 mg/kg) for 4 weeks by intraperitoneal injection. Control (n = 12) and *db/m* (n = 12) mice were administrated with the same volume of vehicle buffer as that for diabetic mice. After 4-week administration of SP6616, mice were killed under sodium pentobarbital (5 mg/100g) anesthesia. Experimenters were blind to assignment of group and assessment of experimental results, and no mice were excluded from the experiments.

Considering that STZ mice at 14-week age and *db/db* mice at 18-week age are old enough accompanying with hypoalgesia at late stage of DPN and our previous work applied 50 mg/kg SP6616 daily by intraperitoneal injection to 8-week old *db/db* mice [26], we thus reduced SP6616 concentrations to 20 and 40 mg/kg in our current experiments.

In addition, given that daily long-term intraperitoneal injection may have impacts on animal stress/welfare [42–44], we detected the related parameters including diet, drinking water, body weight, blood glucose and hormone levels of adrenocorticotropic hormone (ACTH) and corticosterone (CORT) in the serum of Control mice (14-week old C57BL/6J mice, n = 8) and Control + Vehicle (2% DMSO and 8% Tween-80) mice (n = 8). Vehicle was administered daily via intraperitoneal injection for 4 weeks. As indicated in Fig. S3a-f, no significant difference was found for any of the above-mentioned parameters between Control and Control + Vehicle groups.

2.17. Statistical analysis

Data were expressed as mean ± SEM. Two-tailed Student's t test was used to analyze two groups, and one-way ANOVA was used to compare more than two groups by GraphPad Prism 7.0 Software. Data significance analysis was performed as * $P<0.05$, ** $P<0.01$, *** $P<0.001$; $^{\#}P< 0.05$, $^{\#\#}P < 0.01$, $^{\#\#\#}P < 0.001$; ns = no significance.

3. Results

3.1. SP6616 treatment suppressed Kv2.1 expression in DRG tissue of diabetic mice

SP6616 was ever reported to be a selective Kv2.1 inhibitor in our previous work [26]. It inhibited membrane potential in CHO-Kv2.1 cell by IC_{50} at 2.58 μM, and in CHO-Kv2.2 cell by IC_{50} at 13.48 μM. Patch clamp assay also confirmed that SP6616 inhibited Kv2.1 channel by IC_{50} at 6.44 μM.

In the current work, we investigated the level of Kv2.1 expression in DRG tissue of diabetic mice (STZ, *db/db*) by western blot assay. As indicated in Fig. 1b-e, Kv2.1 expression level of DRG tissue was increased in diabetic mice (STZ, *db/db*) compared with that in control mice (Control, *db/m*), and decreased in SP6616-treated diabetic mice (STZ+SP6616, *db/db*+SP6616) compared with that in vehicle-treated diabetic mice (STZ, *db/db*).

Next, immunohistochemistry assay was also performed to detect Kv2.1 expression in DRG tissue of diabetic mice. In the assay, Kv2.1 protein distribution was stained in brown. As indicated in Fig. 1f-i, Kv2.1 expression level in DRG tissue was upregulated from diabetic mice (STZ, *db/db*) compared with that from control mice (Control, *db/m*), and downregulated from SP6616-treated diabetic mice compared with that from vehicle-treated diabetic mice (STZ, *db/db*).

Moreover, we investigated the mRNA levels of Kv2.1 in DRG tissue of diabetic mice (STZ, *db/db*). As indicated in Fig. S4a-b, SP6616 treatment suppressed Kv2.1 mRNA level. We thus tentatively proposed that SP6616 suppressed Kv2.1 expression possibly by reducing the transcription level of Kv2.1channel.

Finally, we also investigated Kv2.2 level in mice. As indicated in Fig. S5a-d, no significant difference was determined for Kv2.2 expression level in DRG tissue between SP6616-treated diabetic mice (STZ+SP6616, *db/db*+SP6616) and vehicle-treated diabetic mice (STZ, *db/db*).

Thus, all the results demonstrated that SP6616 treatment specifically suppressed Kv2.1 expression in DRG tissue of diabetic mice.

3.2. SP6616 treatment enhanced neurite outgrowth of DRG neuron from diabetic mice by inhibiting Kv2.1 channel

Given that axonal damage and degeneration are tightly associated with DPN pathology [45], we inspected the potential regulation of SP6616 treatment against the neurite outgrowth of DRG neuron from diabetic mice by immunostaining assay. As indicated in Fig. 2a-d, the neurite outgrowth of DRG neuron was repressed from diabetic mice (STZ, *db/db*) compared with that from control mice (Control, *db/m*), and enhanced from SP6616-treated diabetic mice (STZ+SP6616, *db/db*+SP6616) compared with that from vehicle-treated diabetic mice (STZ, *db/db*).

Notably, as indicated in Fig. 2e and f, the neurite outgrowth of DRG neuron was obviously upregulated from AAV9-Kv2.1-RNAi injected STZ mice (STZ+AAV9-Kv2.1-RNAi) compared with that from AAV9-NC injected STZ mice (STZ+AAV9-NC), and no significant difference was determined in the neurite outgrowth of DRG neuron between SP6616-treated AAV9-Kv2.1-RNAi injected STZ mice (STZ +AAV9-Kv2.1-RNAi+SP6616) and vehicle-treated AAV9-Kv2.1-RNAi injected STZ mice (STZ+AAV9-Kv2.1-RNAi).

Thus, all the results determined that SP6616 treatment enhanced neurite outgrowth of DRG neuron from diabetic mice by inhibiting Kv2.1 channel.

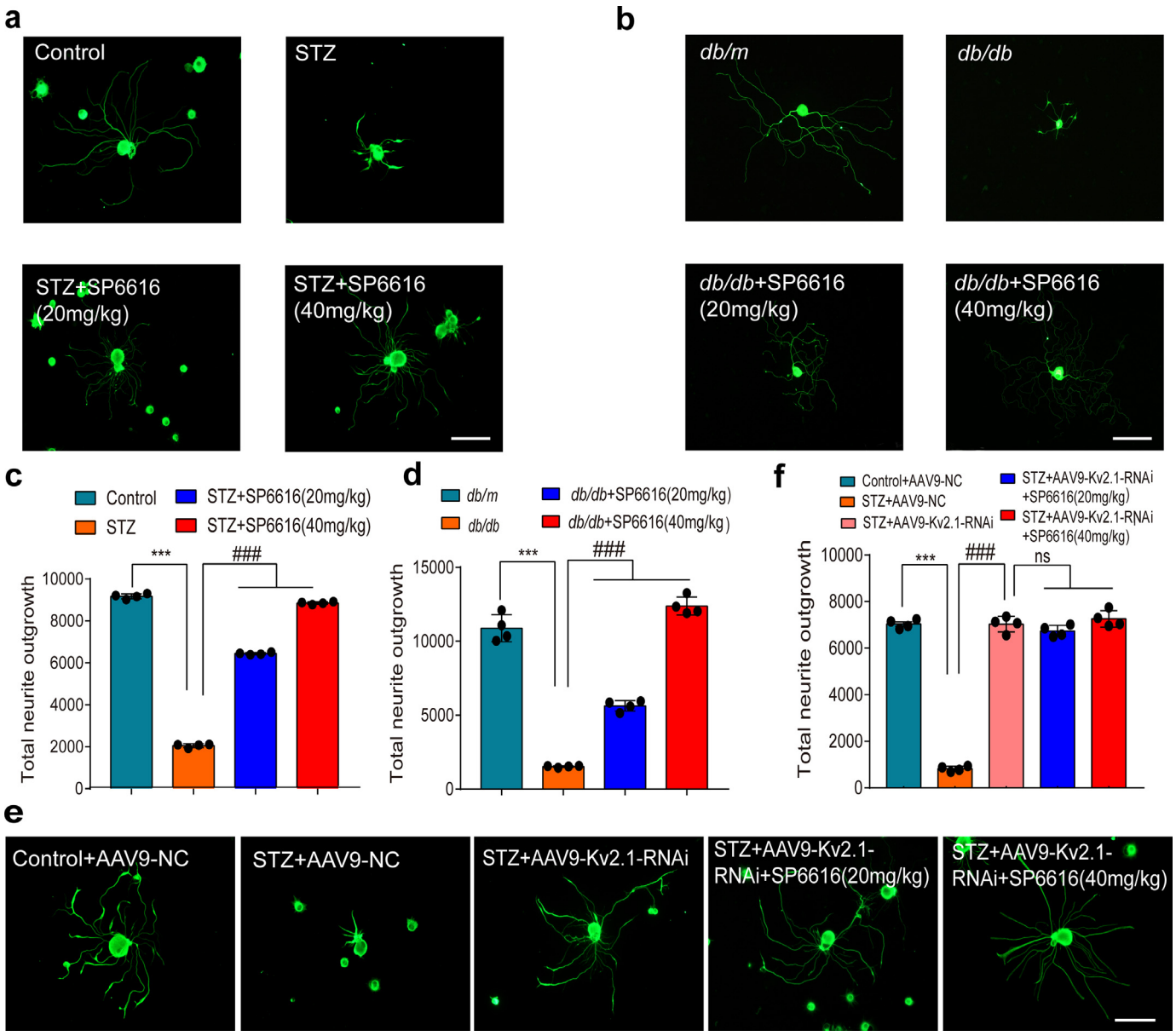

Fig. 2. SP6616 treatment enhanced neurite outgrowth of DRG neuron from diabetic mice by inhibiting Kv2.1 channelβ-tubulin III-immunostained sensory neuron. (**a, b**) Neurite outgrowth of DRG neuron from (**a**) Control, STZ, SP6616 (20, 40 mg/kg)-treated STZ (STZ+20, 40 mg/kg) mice (n = 4), and (**b**) *db/m, db/db* and SP6616 (20, 40 mg/kg)-treated *db/db* (*db/db* + 20, 40 mg/kg) mice (n = 4). (**c, d**) Quantification of the total neurite outgrowth for (**a, b**). (**e**) Neurite outgrowth of DRG neuron from Control, AAV9-negative control (AAV9-NC) injected STZ (STZ+AAV9-NC), AAV9-Kv2.1-RNAi injected STZ (STZ+AAV9-Kv2.1-RNAi) and SP6616 (20, 40 mg/kg)-treated AAV9-Kv2.1-RNAi injected STZ (STZ+AAV9-Kv2.1-RNAi+SP6616) mice (n = 4). (**f**) Quantification of the total neurite outgrowth for (**e**). All the values were presented as mean ± SEM. $^{***}P < 0.001$ *vs* Control or *db/m* (Student's t-test); $^{###}P < 0.001$ *vs* STZ or *db/db* (one-way ANOVA with Dunnett's post-hoc test).

3.3. SP6616 treatment ameliorated peripheral neuropathy of diabetic mice by inhibiting Kv2.1 channel

As indicated in Fig. 3a-f, compared with control mice (Control, *db/m*), diabetic mice (STZ, *db/db*) exhibited typically diabetic peripheral neuropathy features including upregulated levels of 50% paw withdrawal threshold and thermal response latencies, and downregulated level of MNCV. Obviously, SP6616 treatment efficiently ameliorated 50% paw withdrawal threshold (Fig. 3a-b), thermal response latencies (Fig. 3c-d) and MNCV (Fig. 3e-f) in diabetic mice (STZ, *db/db*).

As indicated in Fig. 3g-i, AAV9-Kv2.1-RNAi injected STZ mice (STZ +AAV9-Kv2.1-RNAi) exhibited decreased levels of 50% paw withdrawal threshold and thermal response latencies, and increased level of MNCV compared with AAV9-NC injected STZ mice (STZ+AAV9-NC). Notably, no significant difference was found in the regulation of the above-mentioned behavior parameters between SP6616-treated AAV9-Kv2.1-RNAi injected STZ mice (STZ+AAV9-Kv2.1-RNAi +SP6616) and vehicle-treated AAV9-Kv2.1-RNAi injected STZ mice (STZ+AAV9-Kv2.1-RNAi).

In addition, by considering that our previously published report demonstrated that SP6616 could ameliorate blood glucose homeostasis in type 2 diabetic mice [26], we here also investigated the potential effect of SP6616 on the blood glucose homeostasis in mice. As indicated in Fig. S6a-f, SP6616 treatment had no effects on body weight or fasting blood glucose in diabetic mice (STZ, *db/db*) or AAV9-Kv2.1-RNAi injected STZ mice. Also, we inspected the potential regulation of insulin in responding to the SP6616-mediated amelioration on DPN-like pathology, but the results in Fig. S6g-h indicated that SP6616 treatment had no effects on insulin level in diabetic mice (STZ, *db/db*).

Finally, the potential regulation of SP6616 against sensory sensitivity and electrophysiological activity in non-diabetic mice (Control,

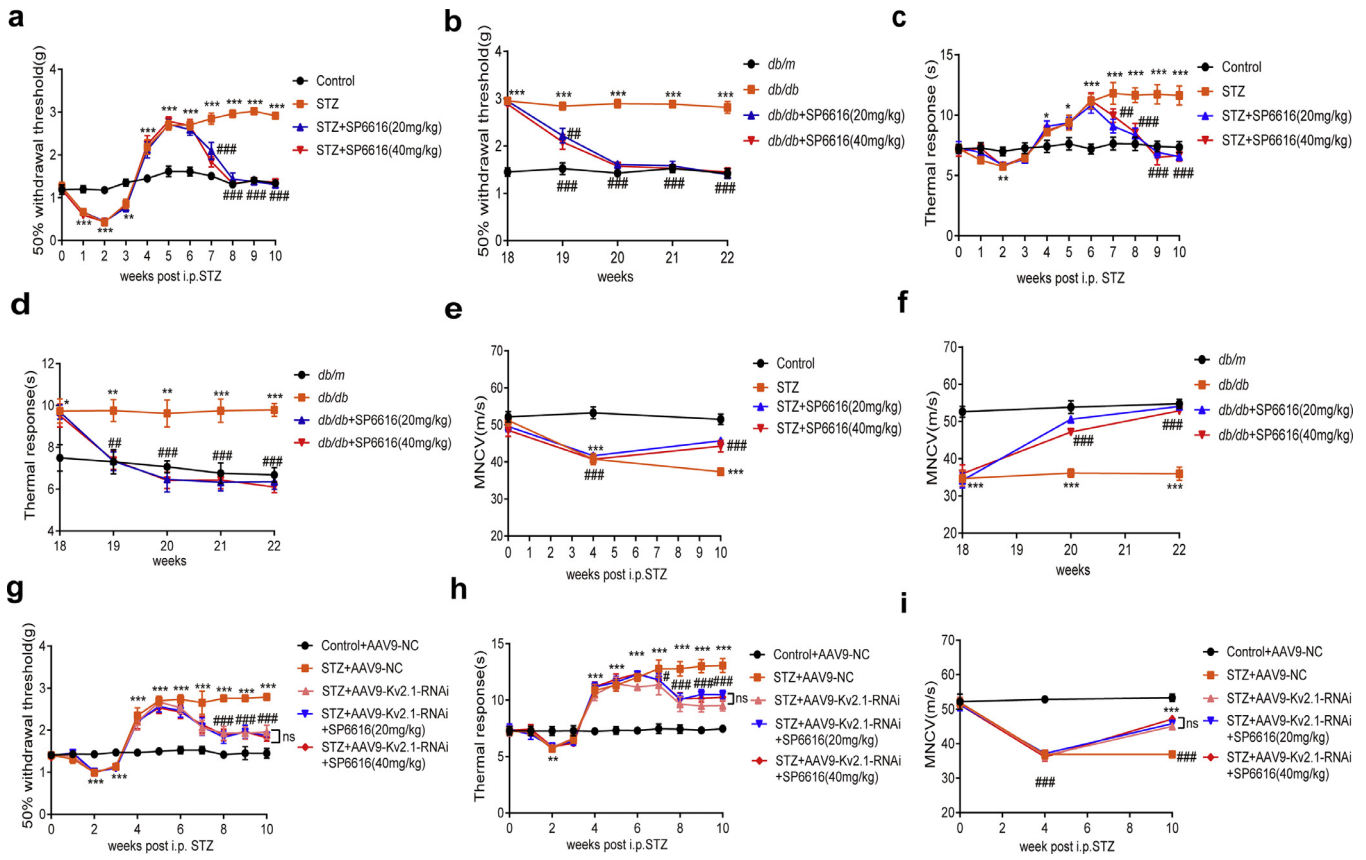

Fig. 3. SP6616 treatment ameliorated peripheral neuropathy in diabetic mice by inhibiting Kv2.1 channel(**a, b**) SP6616 (20, 40 mg/kg) treatment ameliorated 50% mechanical threshold in (**a**) STZ (n = 12) and (**b**) *db/db* mice (n = 12). (**c, d**) SP6616 (20, 40 mg/kg) treatment improved paw thermal response latency in (**c**) STZ (n = 12) and (**d**) *db/db* mice (n = 12). (**e, f**) SP6616 (20, 40 mg/kg) treatment enhanced MNCV in (**e**) STZ (n = 12) and (**f**) *db/db* mice (n = 12). (**g, h, i**) No significant difference was found in the amelioration of (**g**) tactile allodynia (**h**) thermal sensitivity (**i**) MNCV between SP6616 (20, 40 mg/kg)-treated AAV9-Kv2.1-RNAi injected STZ mice (STZ+AAV9-Kv2.1-RNAi+SP6616; n = 12) and vehicle-treated AAV9-Kv2.1-RNAi injected STZ mice (STZ+AAV9-Kv2.1-RNAi; n = 12). All the values were presented as mean ± SEM. $^{*}P<0.05$, $^{**}P < 0.01$, $^{***}P < 0.001$ *vs* non-diabetic mice (Control or *db*/m) (Student's t-test); $^{\#}P< 0.05$, $^{\#\#}P < 0.01$, $^{\#\#\#}P < 0.001$ *vs* diabetic mice (STZ or *db/db* mice) (one-way ANOVA with Dunnett's post-hoc test).

14-week old C57BL/6J) was inspected. In the assay, tactile allodynia, thermal sensitivity, MNCV, body weight and blood glucose were detected against the mice treated with SP6616 (20, 40 mg/kg) for 4 weeks. As shown in Fig. S7a-e, SP6616 had no impacts on any of these parameters in nondiabetic mice.

Thus, all the results demonstrated that SP6616 treatment ameliorated peripheral neuropathy in diabetic mice by inhibiting Kv2.1 channel.

3.4. SP6616 treatment improved peripheral nerve structure and vascular function in diabetic mice

Given that reduced MNCV and impaired sensory response are accompanied with intraepithelial nerve fibers (IENF) loss in DPN progression [35, 46], we detected the number of fibers in foot pads of diabetic mice by immunohistochemical staining assay. As shown in Fig. 4a-c, the number of fibers in foot pads was downregulated in diabetic mice (STZ, *db/db*) compared with that in control mice (Control, *db/m*), and upregulated in SP6616-treated diabetic mice (STZ +SP6616, *db/db*+SP6616) compared with that in vehicle-treated diabetic mice (STZ, *db/db*).

As indicated in the published reports, vascular structural changes are severely involved in DPN and other microvascular diseases [29] and microvascular dysfunction induces peripheral nerve flow hypoperfusion that is also tightly associated with DPN [4, 47]. We thus examined the vascular function in sciatic nerve and foot pads of mice by detecting blood flow velocity and blood perfusion area through Laser Speckle Contrast Imaging. As indicated in Fig. 4d-k, the blood flow velocity and blood perfusion area were repressed in diabetic mice (STZ, *db/db*) compared with those in control mice (Control, *db/m*), and ameliorated in SP6616-treated diabetic mice (STZ+SP6616, *db/db*+SP6616) compared with those in vehicle-treated diabetic mice (STZ, *db/db*).

Thus, all results demonstrated that SP6616 improved peripheral nerve structure and vascular function in diabetic mice.

3.5. SP6616 treatment improved mitochondrial dysfunction of DRG neuron in diabetic mice through Kv2.1/CaMKKβ/AMPK/PGC-1α pathway

SP6616 improved mitochondrial dysfunction by inhibiting Kv2.1 channel- Given that oxygen consumption rate (OCR) as a key indicator assesses mitochondrial bioenergetics and metabolic functions of cell [20, 46], the potential regulation of SP6616 treatment against OCR was detected in DRG neuron from diabetic mice via Seahorse Biosciences XF96 analyzer. As SP6616 at 20 mg/kg already performed appreciably therapeutic effects (tactile allodynia, thermal sensitivity and MNCV) on diabetic mice (Fig. 3a-f), the assay was carried out against the sample at 20 mg/kg for experiment convenience.

The results indicated that the levels of OCR (Fig. 5a-b), basal respiration (Fig. 5c-d), ATP production (Fig. 5e-f), maximum respiration (Fig. 5g-h) and spare capacity (Fig. 5i-j) in DRG neuron were all downregulated from diabetic mice (STZ, *db/db*) compared with those from control mice (Control, *db/m*), and all upregulated from SP6616-treated diabetic mice (STZ+SP6616, *db/db*+SP6616) compared with those from vehicle-treated diabetic mice (STZ, *db/db*).

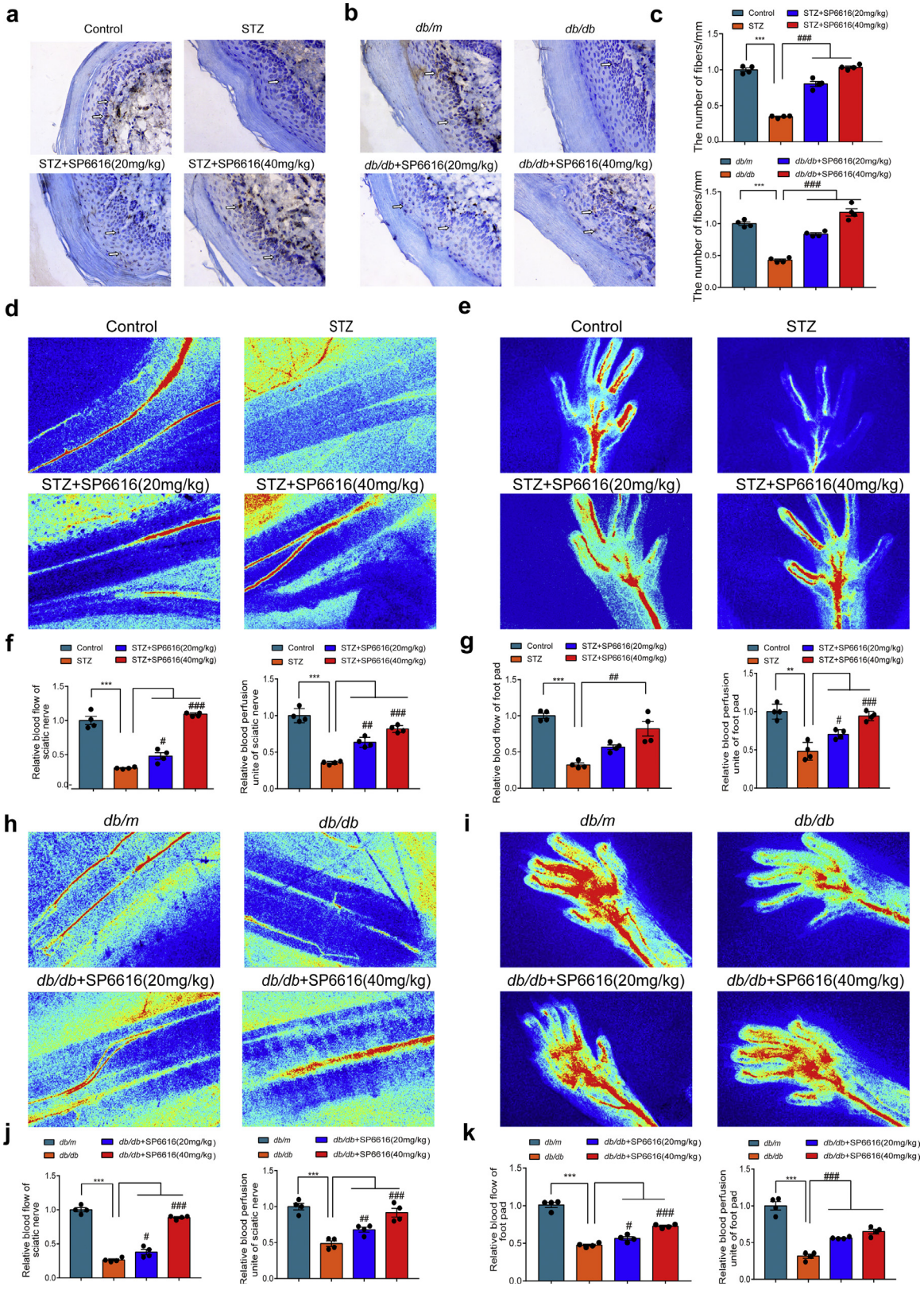

Fig. 4. SP6616 treatment increased the number of fibers in foot pads and promoted neurovascular function in diabetic micePGP9.5 antibody labeled nerve fibers and hematoxylin labeled nucleus. (**a, b**) Representative images of intraepidermal nerve fiber (IENF) in hind paw plantar skin of (**a**) Control, STZ and SP6616 (20, 40 mg/kg)-treated STZ (STZ + 20, 40 mg/kg) mice (n = 4), and (**b**) *db/m, db/db* and SP6616 (20, 40 mg/kg)-treated *db/db* (*db/db* + 20, 40 mg/kg) mice (n = 4). (**c**) Quantification of the number of fibers/mm in hind paw plantar skin for (**a, b**). (**d, e**) Representative images of regional blood flow velocity and perfusion ratios in (**d**) sciatic nerve and (**e**) foot pad tissues of Control, STZ and SP6616 (20, 40 mg/kg)-treated STZ (STZ + 20, 40 mg/kg) mice (n = 4). (**f, g**) Quantification for (**d, e**). (**h, i**) Representative images of regional blood flow velocity and perfusion ratios in (**h**) sciatic nerve and (**i**) foot pad tissues of *db/m, db/db* and SP6616 (20, 40 mg/kg)-treated *db/db* (*db/db* + 20, 40 mg/kg) mice (n = 4). (**j, k**) Quantification for (**h, i**). All the data were normalized by blood flow velocity and perfusion ratios in sciatic nerve or foot pad tissues from Control or *db*/m presented as mean ± SEM. Lowest blood flow was in blue and maximum blood flow was in red. $^{**}P < 0.01$, $^{***}P < 0.001$ *vs* Control or *db/m* (Student's t-test); $^{\#}P < 0.05$; $^{\#\#}P < 0.01$; $^{\#\#\#}P < 0.001$ *vs* diabetic mice (STZ, *db/db*) (one-way ANOVA with Dunnett's post-hoc test).

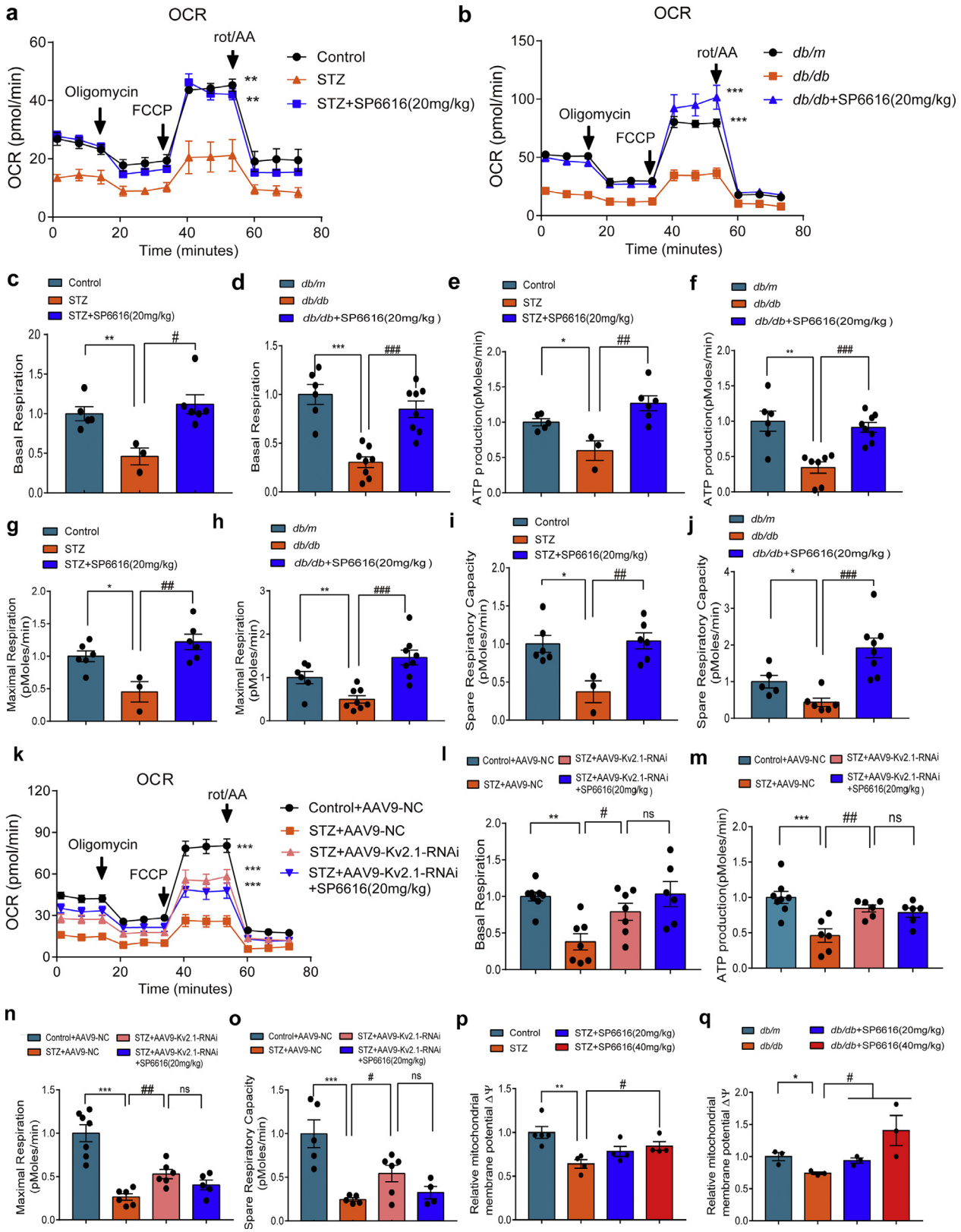

Fig. 5. SP6616 treatment improved abnormal mitochondrial respiration in DRG neuron from diabetic mice by inhibiting Kv2.1 channelOxygen consumption rate (OCR) was measured at basal level with sequential addition of oligomycin (1 μM), FCCP (1 μM) and rotenone (1 μM) with antimycin A (AA; 1 μM) to DRG neuron from Control (n = 5-6), *db/m* (n = 5-6), STZ (n = 3), *db/db* (n = 6-8) and SP6616 (20 mg/kg)-treated STZ (STZ + 20 mg/kg, n = 6; *db/db* + 20 mg/kg, n = 8) mice. SP6616 (20 mg/kg) treatment enhanced (**a, b**) OCR, (**c, d**) basal respiration, (**e, f**) ATP production, (**g, h**) maximal respiration and (**i, j**) spare respiratory capacity in diabetic mice. (**k-o**) SP6616 treatment failed to affect (**k**) OCR, (**l**) basal respiration, (**m**) ATP production, (**n**) maximal respiration and (**o**) spare respiratory capacity in AAV9-Kv2.1-RNAi injected STZ mice (STZ+AAV9-Kv2.1-RNAi+SP6616) (n = 4-6) by comparing with the corresponding results in vehicle-treated AAV9-Kv2.1-RNAi injected STZ mice (STZ+AAV9-Kv2.1-RNAi) (n = 6-7). Mitochondrial inner membrane potential (MMP) level in neuron from (**p**) Control, STZ and SP6616 (20, 40 mg/kg)-treated STZ (STZ+20, 40 mg/kg) mice (n = 4), and (**q**) *db/m, db/db* and SP6616 (20, 40 mg/kg)-treated *db/db* (*db/db*+20, 40 mg/kg) mice (n = 3). MMP level was presented as a ratio of aggregate to monomer. Monomer indicates early apoptosis and aggregate indicates normal state. All the values were presented as mean ± SEM; *P<0.05, **P < 0.01, ***P < 0.001 *vs* Control or *db/m* (Student's t-test); $^{\#}$P< 0.05; $^{\#\#}$P < 0.01; $^{\#\#\#}$P < 0.001 *vs* STZ or *db/db* (Student's t-test).

Notably, as indicated in Fig. 5k-o, the levels of the above-mentioned five parameters of DRG neuron were all upregulated from AAV9-Kv2.1-RNAi injected STZ mice (STZ+AAV9-Kv2.1-RNAi) compared with those from AAV9-NC injected STZ mice (STZ+AAV9-NC), and no significant difference was found in the level of any of the above parameters of DRG neuron between SP6616-treated AAV9-Kv2.1-RNAi injected diabetic mice (STZ+AAV9-Kv2.1-RNAi+SP6616) and vehicle-treated AAV9-Kv2.1-RNAi injected diabetic mice (STZ +AAV9-Kv2.1-RNAi).

Thus, all the results demonstrated that SP6616 improved mitochondrial dysfunction through inhibiting Kv2.1 channel.

SP6616 treatment ameliorated MMP level of DRG neuron from diabetic mice- In addition, we also detected the level of mitochondrial membrane potential (MMP) in DRG neuron from SP6616-treated or -untreated diabetic mice by fluorescent probe JC-1. As indicated in Fig. 5p-q, MMP level of DRG neuron from SP6616-treated diabetic mice (STZ+SP6616, *db/db*+SP6616) was upregulated compared with that from vehicle-treated diabetic mice (STZ, *db/db*). These results thereby demonstrated that SP6616 treatment ameliorated MMP level of DRG neuron in diabetic mice.

SP6616 improved mitochondrial function by regulating Kv2.1/CaMKKβ/AMPK/PGC-1α pathway- It was noted that Kv inhibition increased calcium flux by directly activating CaMKKβ [48]. Here we also determined that SP6616 promoted intracellular Ca^{2+} level by assay with nifedipine as the known calcium channel inhibitor (Fig. 6a-e).

As shown in Fig. 6f-i, the protein levels of CaMKKβ, phosphorylated AMPK, phosphorylated ACC (direct substrate of AMPK) and PGC-1α of DRG tissue were upregulated in SP6616-treated diabetic mice (STZ+SP6616, *db/db*+SP6616) compared with those in vehicle-treated diabetic mice (STZ, *db/db*). Notably, no significant difference was found in any of these above-mentioned four protein levels in DRG tissue between SP6616-treated AAV9-Kv2.1-RNAi injected STZ mice (STZ+AAV9-Kv2.1-RNAi+SP6616) and vehicle-treated AAV9-Kv2.1-RNAi injected STZ mice (STZ+ AAV9-Kv2.1-RNAi) (Fig. 6j-k).

Together, SP6616 improved mitochondrial function by regulating Kv2.1/CaMKKβ/AMPK/PGC-1α signaling pathway.

3.6. SP6616 treatment repressed inflammation in diabetic mice by inhibiting Kv2.1/NF-κB signaling

SP6616 suppressed proinflammatory cytokines in the serum of diabetic mice- Given the tight association of inflammation with DPN pathology [49, 50], we investigated the regulation of SP6616 treatment against inflammation in diabetic mice. ELISA assay results (Fig. 7a-f) indicated that the levels of proinflammatory cytokines TNF-α, IL-1β and IL-6 were downregulated in the serum of SP6616-treated diabetic mice (STZ+SP6616, *db/db*+SP6616) compared with those of vehicle-treated diabetic mice (STZ, *db/db*).

In addition, western blot results (Fig. 7g-j) also demonstrated that protein levels of inflammatory cytokines TNF-α and iNOS of DRG tissue were both downregulated from SP6616-treated diabetic mice (STZ+SP6616, *db/db*+SP6616) compared with those from vehicle-treated diabetic mice (STZ, *db/db*).

SP6616 repressed inflammation of DRG neuron in diabetic mice by regulating Kv2.1/NF-κB signaling- Since NF-κB as a nuclear transcription factor functions potently in regulating a large number of genes critical for regulation of inflammation including inflammatory cytokines IL-6, IL-1β and TNF-α [51], we investigated the potential regulation of SP6616 against NF-κB signaling in DRG neuron from mice by immunohistochemistry assay.

As indicated in Fig. 7k-o, the intensity of red fluorescence (NF-κB) in nuclear of DRG neuron was upregulated from diabetic mice (STZ, *db/db*) compared with that from control mice (Control, *db/m*), and obviously decreased from SP6616-treated diabetic mice (STZ +SP6616, *db/db*+SP6616) compared with that from vehicle-treated diabetic mice (STZ, *db/db*). These results thus demonstrated that SP6616 treatment promoted NF-κB translocation from nucleus to cytoplasm, indicative of the suppression of inflammation. Notably, no significant difference was found for the intensity level of red fluorescence (NF-κB) in nuclear of DRG neuron between SP6616-treated AAV9-Kv2.1-RNAi injected STZ mice (STZ+AAV9-Kv2.1-RNAi +SP6616) and vehicle-treated AAV9-Kv2.1-RNAi injected STZ mice (STZ+AAV9-Kv2.1-RNAi).

In addition, considering that p-IκBα stimulates NF-κB/p65 translocation into nucleus [52], we also examined the potential of SP6616 in regulating p-IκBα by western blot. As indicated in Fig. 7g-j, p-IκBα level in DRG tissue was decreased from SP6616-treated diabetic mice (STZ+SP6616, *db/db*+SP6616) compared with that from vehicle-treated diabetic mice (STZ, *db/db*). Notably, no significant difference was found in the protein levels of p-IκBα, TNF-α and iNOS in DRG tissue between SP6616-treated AAV9-Kv2.1-RNAi injected STZ mice (STZ+AAV9-Kv2.1-RNAi+SP6616) and vehicle-treated AAV9-Kv2.1-RNAi injected STZ mice (STZ+AAV9-Kv2.1-RNAi) (Fig. 7p and q).

Therefore, all the data demonstrated that SP6616 treatment inhibited inflammation of diabetic mice by regulating Kv2.1/NF-κB signaling.

3.7. SP6616 protected peripheral neuron from apoptosis involving regulation of Bcl-2 family proteins and Caspase-3 in diabetic mice by inhibiting Kv2.1 channel

Kv2.1 channel is tightly linked to the regulation of potassium homeostasis and abnormal potassium homeostasis causes sustained outflow of potassium ions leading to disorder, dysfunction and a series of apoptotic cascades of cells [53], which are highly associated with DPN pathology. With these facts, we inspected the potential of SP6616 treatment in preventing against the apoptosis of DRG neuron from diabetic mice.

SP6616 treatment prevented DRG neuron from apoptosis in diabetic mice - As shown in Fig. 8a-d, DRG neuron from diabetic mice (STZ, *db/db*) showed increased intensity of green fluorescence (apoptotic cell) compared with that from control mice (Control, *db/m*). Obviously, DRG neuron from SP6616-treated diabetic mice (STZ+SP6616, *db/db* +SP6616) exhibited decreased intensity of apoptotic cell compared with that from vehicle-treated diabetic mice (STZ, *db/db*). Thus, all results suggested that SP6616 treatment prevented against the apoptosis of DRG neuron in diabetic mice.

SP6616 protected DRG neuron from apoptosis involving regulation of Bcl-2 family proteins and Caspase-3 by inhibiting Kv2.1 channel- Given that Bcl-2 family proteins and Caspase-3 are vital regulators of apoptosis [54, 55], western blot assay was carried out against these proteins in DRG tissue from mice. As indicated in Fig. 8e-j, the DRG tissue from SP6616-treated diabetic mice (STZ+SP6616, *db/db* +SP6616) exhibited decreased levels of pro-apoptotic proteins (Cleaved-caspase 3, Bax) and increased levels of anti-apoptotic proteins (Bcl-2, Bcl-xl, p-Bad) (Bad with anti-apoptotic effect after phosphorylation [56]) compared with that from vehicle-treated diabetic mice (STZ, *db/db*). Notably, no significant difference was determined in the regulation of pro-apoptotic or anti-apoptotic proteins of DRG tissue between SP6616-treated AAV9-Kv2.1-RNAi injected STZ mice (STZ+AAV9-Kv2.1-RNAi+SP6616) and vehicle-treated AAV9-Kv2.1-RNAi injected STZ mice (STZ+AAV9-Kv2.1-RNAi).

Taken together, all the results implied that SP6616 protected DRG neuron from apoptosis involving regulation of Bcl-2 family proteins and Caspase-3 by inhibiting Kv2.1 channel.

4. Discussion

DPN is a commonly long-term diabetic complication with complicated etiology, and there is yet no effective medication to treat this

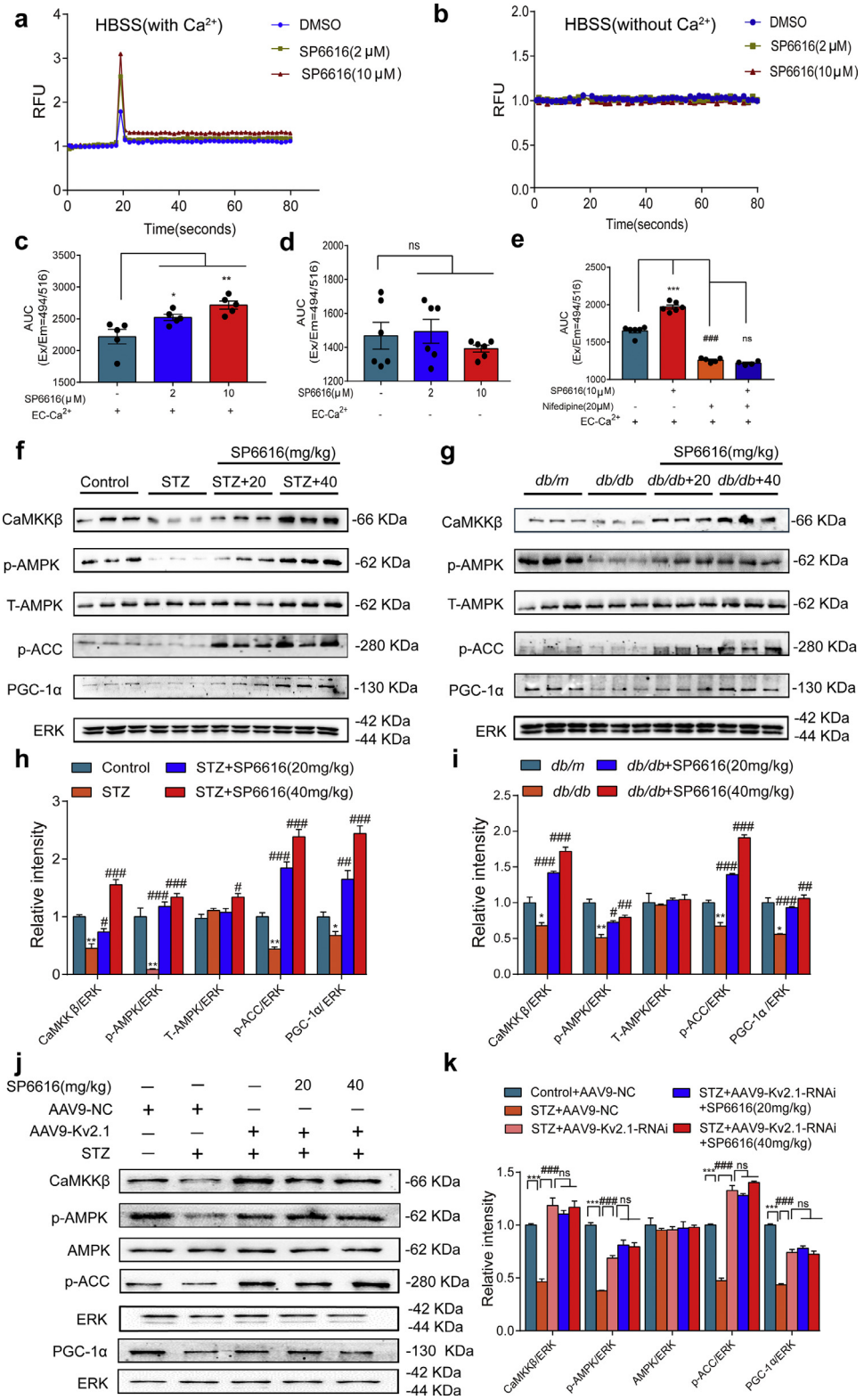

Fig. 6. SP6616 treatment promoted Kv2.1/CaMKKβ/AMPK/PGC-1α pathway by inhibiting Kv2.1 channel(**a, b**) Fluo-4 AM assay was used to detect the effect of SP6616 on Ca^{2+} level in DRG neuron from adult C57BL/6J mice. The curve represented the calcium signal value at each time point, and the baseline fluorescence signal was measured for the first 20s. SP6616 (2, 10 μM) was added by FlexStation 3. (**a**) SP6616 (2, 10 μM) promoted calcium influx in HBSS buffer with Ca^{2+}. (**b**) SP6616 (2, 10 μM) had no effects on calcium signal in HBSS buffer without Ca^{2+}. (**c**) The area under the curve (AUC) corresponding to (**a**) (n = 5). (**d**) AUC corresponding to (**b**) (n = 6). (**e**) The intracellular Ca^{2+} assay with nifedipine (known calcium channel antagonist) was detected in HBSS buffer with Ca^{2+}. AUC represented intracellular calcium signal (n = 4-6). (**f, g**) Quantitative immunoblot analysis revealed that the expression levels of CaMKKβ, p-AMPK, phosphorylated acetyl CoA carboxylase (p-ACC) and PGC-1α were reduced in STZ and *db/db* mice versus Control and *db/m* mice, and upregulated in SP6616 (20, 40 mg/kg)-treated diabetic mice (STZ + 20, 40 mg/kg; *db/db* + 20, 40 mg/kg) versus vehicle-treated diabetic mice (STZ, *db/db*). (**h, i**) Quantification of protein expression for (**f**) and (**g**). (**j**) SP6616 (20, 40 mg/kg) treatment had no effects on CaMKKβ/AMPK/PGC-1α pathway in AAV9-Kv2.1-RNAi injected STZ mice (STZ+AAV9-Kv2.1-RNAi+SP6616) by comparing with the corresponding results in vehicle-treated AAV9-Kv2.1-RNAi injected STZ mice (STZ+AAV9-Kv2.1-RNAi) (n = 3). (**k**) Quantification of protein expression for (**j**). All expressions were normalized to T-ERK level. All the values were presented as mean ± SEM. $^{*}P < 0.05$, $^{**}P < 0.01$, $^{***}P < 0.001$ *vs* Control or *db/m* (Student's t-test); $^{\#}P < 0.05$, $^{\#\#}P < 0.01$, $^{\#\#\#}P < 0.001$ *vs* STZ or *db/db* (one-way ANOVA with Dunnett's post-hoc test).

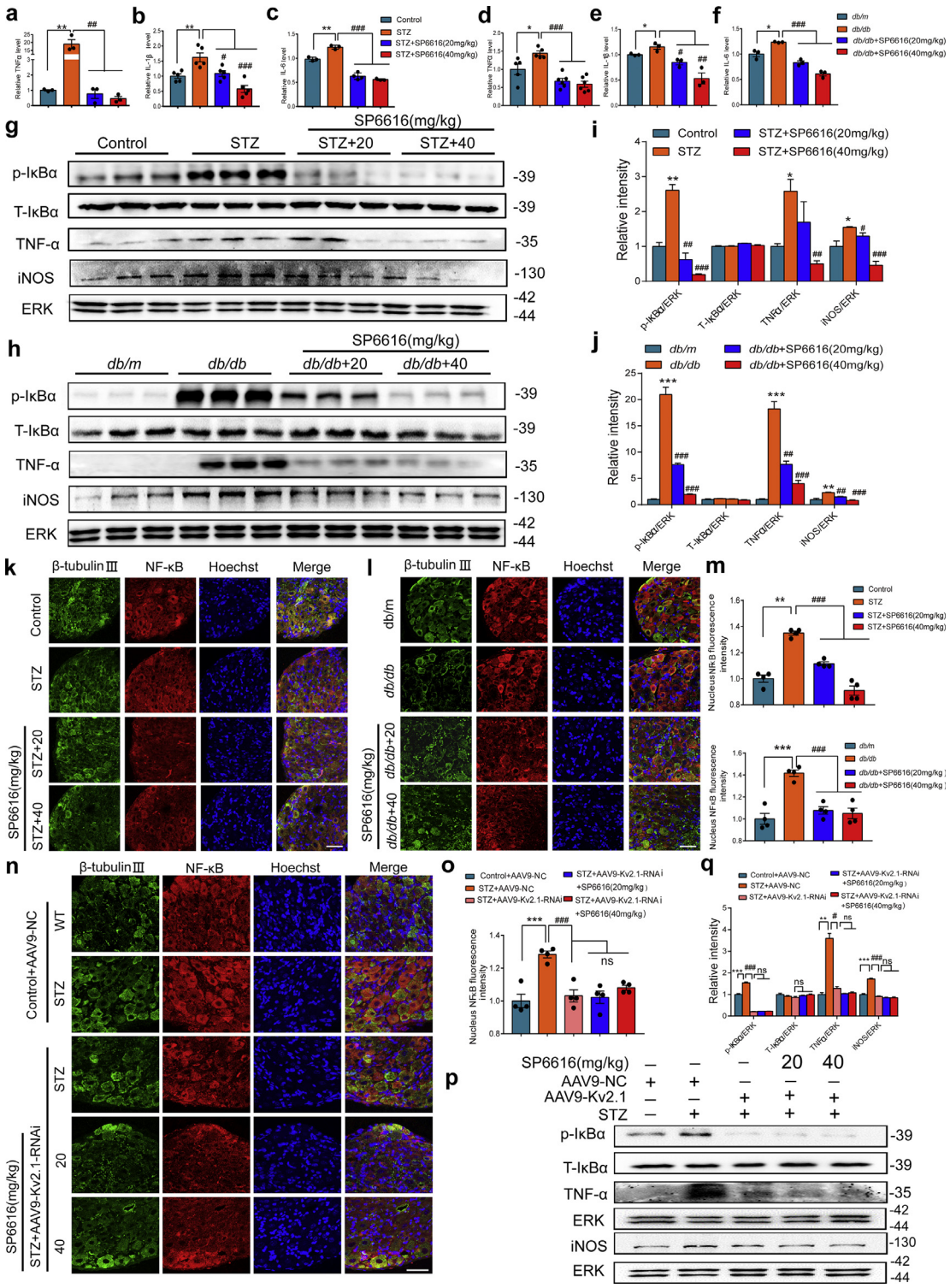

Fig. 7. SP6616 treatment downregulated proinflammatory cytokines involving Kv2.1/NF-κB signaling pathway by inhibiting Kv2.1 channelLevels of (**a**) TNF-α, (**b**) IL-1β and (**c**) IL-6 in the serum of Control (n = 3, 5, 3, respectively), STZ (n = 3, 5, 3, respectively) and SP6616 (20, 40 mg/kg)-treated STZ (STZ + 20, 40 mg/kg) mice (n = 3, 5, 3-4, respectively). Levels of (**d**) TNF-α, (**e**) IL-1β and (**f**) IL-6 in the serum of *db/m* (n = 5, 3, 3, respectively), *db/db* (n = 5, 3, 3, respectively) and SP6616 (20, 40 mg/kg)-treated *db/db* (*db/db* + 20, 40 mg/kg) mice (n = 6, 3, 3, respectively). (**g, h**) Quantitative immunoblot analysis revealed the expressions of p-IκBα, TNF-α and iNOS from (**g**) Control, STZ and SP6616 (20, 40 mg/kg)-treated STZ (STZ+20, 40 mg/kg) mice (n = 3), and (**h**) *db/m*, *db/db* and SP6616 (20, 40 mg/kg)-treated *db/db* (*db/db*+20, 40 mg/kg) mice (n = 3). (**i, j**) Quantification of protein expression for (**g, h**). (**k, l**) Representative immuno-fluorescent images showing neuron-specific β-tubulin isotype III (neuron, green), NF-κB (NF-κB antibody, red) and Hoechst (nucleus, blue) staining in DRG sections from (**k**) Control, STZ and SP6616 (20, 40 mg/kg)-treated STZ (STZ+20, 40 mg/kg) mice (n = 4), and (**l**) *db/m, db/db* and SP6616 (20, 40 mg/kg)-treated *db/db* (*db/db*+20, 40 mg/kg) mice (n = 4). (**m**) Quantification of nucleus NF-κB fluorescence intensity for (**k, l**). (**n**) Representative immuno-fluorescent images showing neuron-specific β-tubulin isotype III (neuron, green), NF-κB (NF-κB antibody, red) and Hoechst (nucleus, blue) staining in DRG sections from AAV9-NC injected STZ (STZ+AAV9-NC), AAV9-Kv2.1-RNAi injected STZ (STZ+AAV9-Kv2.1-RNAi) and SP6616 (20, 40 mg/kg)-treated AAV9-Kv2.1-RNAi injected STZ (STZ+AAV9-Kv2.1-RNAi+20, 40 mg/kg) mice (n = 4). (**o**) Quantification of nucleus NF-κB fluorescence intensity for (**n**). (**p**) Representative immuno-fluorescent images showing the expressions of p-IκBα, TNF-α and iNOS from AAV9-NC injected STZ (STZ +AAV9-NC), AAV9-Kv2.1-RNAi injected STZ (STZ+AAV9-Kv2.1-RNAi) and SP6616 (20, 40 mg/kg)-treated AAV9-Kv2.1-RNAi injected STZ (STZ+AAV9-Kv2.1-RNAi+20, 40mg/kg) mice (n = 3). (**q**) Quantification of protein expression for (**p**). All the expressions were normalized to T-ERK level in western blot assay. All the values were presented as mean ± SEM; $^{*}P < 0.05$, $^{**}P < 0.01$, $^{***}P < 0.001$ *vs* Control or *db/m* (Student's t-test); $^{\#}P < 0.05$, $^{\#\#}P < 0.01$, $^{\#\#\#}P < 0.001$ *vs* STZ or *db/db* (one-way ANOVA with Dunnett's post-hoc test).

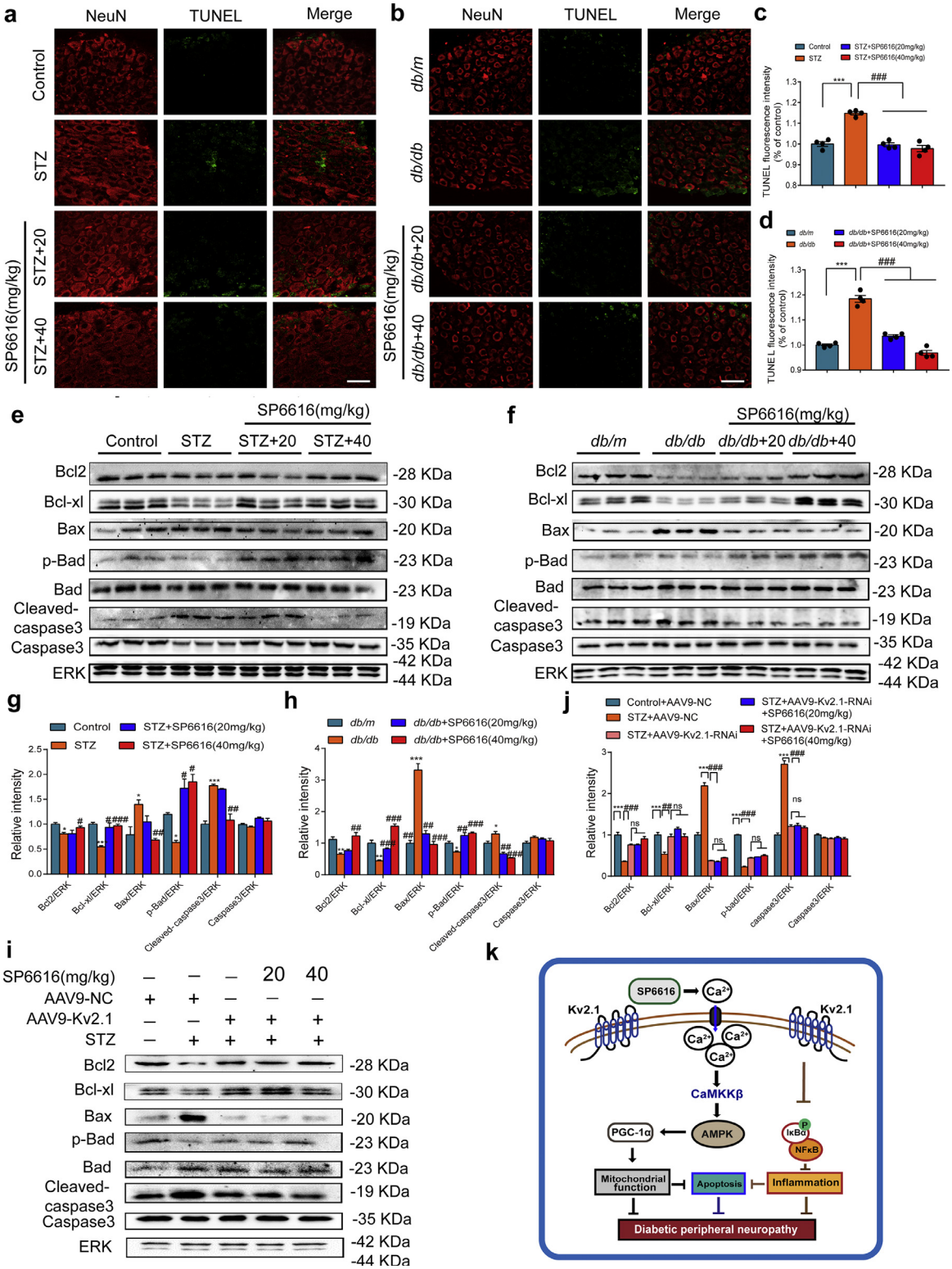

Fig. 8. SP6616 treatment protected DRG neuron from apoptosis involving regulation of Bcl-2 family proteins and Caspase-3 by inhibiting Kv2.1 channel in diabetic mice(**a, b**) TUNEL assays in DRG tissue from (**a**) Control, STZ and SP6616 (20, 40 mg/kg)-treated STZ (STZ+20, 40 mg/kg) (n = 4), and (**b**) *db/m*, *db/db* and SP6616 (20, 40 mg/kg)-treated *db/db* (*db/db* +20, 40 mg/kg) mice (n = 4). Apoptotic DRG neuron was labeled with TUNEL (green fluorescence). The results demonstrated that SP6616 treatment improved neuronal survival in diabetic mice. (**c, d**) Quantification of fluorescence intensity for (**a, b**). (**e, f**) Quantitative immunoblot analysis revealed the expressions of Bcl-2, Bcl-xl, Bax, p-Bad and Cleaved-caspase 3 in DRG neuron from (**e**) Control, STZ and SP6616 (20, 40 mg/kg)-treated STZ (STZ+20, 40 mg/kg) mice (n = 3), and (**f**) *db/m*, *db/db* and SP6616 (20, 40 mg/kg)-treated *db/db* (*db/db*+20, 40 mg/kg) mice (n = 3). (**g, h**) Quantification of protein expression for (**e, f**). (**i**) Quantitative immunoblot analysis revealed the expressions of Bcl-2, Bcl-xl, Bax, p-Bad and Cleaved-caspase 3 in DRG neuron from AAV9-NC injected STZ (STZ+AAV9-NC), AAV9-Kv2.1-RNAi injected STZ (STZ+AAV9-Kv2.1-RNAi) and SP6616 (20, 40 mg/kg)-treated AAV9-Kv2.1-RNAi injected STZ (STZ+AAV9-Kv2.1-RNAi+20, 40mg/kg) mice (n = 3). (**j**) Quantification of protein expression for (**i**). (**k**) SP6616 treatment ameliorated mitochondrial dysfunction, suppressed inflammation and alleviated apoptosis in DRG neuron from diabetic mice. All the expressions were normalized to T-ERK level in western blot assay. All the values were presented as mean ± SEM. $^{*}P < 0.05$, $^{**}P < 0.01$, $^{***}P < 0.001$ *vs* Control or *db/m* (Student's t-test); $^{\#}P < 0.05$, $^{\#\#}P < 0.01$, $^{\#\#\#}P < 0.001$ *vs* STZ or *db/db* (one-way ANOVA with Dunnett's post-hoc test).

disease. It is full of challenges to design new type of reagents against DPN based on new strategies and targets [9].

ATP is necessary for neurite outgrowth of DRG neuron, and deficiency of nutrients aggravates the reduction of axon growth, blockage of conduction, and retraction of distal nerve endings [57]. Here, we determined that SP6616 as a Kv2.1 inhibitor efficiently enhanced neurite outgrowth of DRG neuron in diabetic mice, thus strengthening the potency of Kv2.1 channel in energy homeostasis and the regulation of neurite outgrowth of DRG neuron, further highlighting the potential of SP6616 in the treatment of DPN.

Abnormal calcium homeostasis is tightly associated with varied diseases, including diabetes and DPN [58, 59], and calcium release participates in a lot of physiological events such as neurotransmitter, hormone secretion, synaptic plasticity and mitochondrial function. Reduced calcium signal in DRG neuron of diabetic mice induces axonal nutrient deficiency and mitochondrial dysfunction that are highly responsible for DPN etiology [59, 60]. Here, SP6616 as a Kv2.1 inhibitor ameliorated mitochondrial dysfunction and ATP generation in DRG neuron of diabetic mice by stimulating intracellular Ca^{2+} release through opening the voltage-dependent Ca^{2+} channels (VDCCs) and activating CaMKKβ/AMPK/PGC-1α signaling. Our work has expounded the potential mechanism underlying the amelioration of Kv2.1 inhibition on mitochondrial function in diabetic mice by using SP6616 as a probe.

NF-κB and inflammatory cytokines are main contributors for neurovascular damage and nerve conduction velocity impairment in DPN [61]. SP6616 was determined to repress proinflammatory cytokines TNF-α, IL-1β and IL-6 through Kv2.1/NF-κB signaling in diabetic mice. In addition, peripheral sensory neuron loss is accompanied with the occurrence of apoptosis, which is also a major cause for DPN [24, 62]. Here, we found that SP6616 treatment efficiently protected against neuronal apoptosis, thereby supporting that inhibition of Kv2.1 channel might be also a potential strategy for treating other inflammation and apoptosis-related diseases.

Moreover, neurovascular dysfunction is tightly associated with DPN pathology, and published results have indicated that inflammation reduction promotes the recovery of vascular function [63, 64]. In the current work, we have also found that SP6616 effectively improved peripheral blood perfusion and alleviated intraepithelial nerve fibers loss. Here, we tentatively suggested that such a neurovascular function improvement may result from the anti-inflammatory effect of SP6616.

It was noticed that apart from DRG tissue, sciatic nerve and spinal cord also participate in the regulation of DPN pathology. For example, sciatic nerve involves neurovascular and peripheral nerve functions [65–67] and spinal cord is implicated in sensory information processing [68–70]. By assay against the STZ mice injected with AAV9-Kv2.1-RNAi, we determined that different from the case for Kv2.2 where Kv2.2 was independent of AAV9-Kv2.1-RNAi injection in any of the three tissues of the mice (DRG, sciatic nerve and spinal cord), Kv2.1 expression level was repressed by almost the same degree in these three tissues (Fig. S8a-h). Thus, we proposed that amelioration of SP6616 on DPN-like pathology in diabetic mice should benefit from its Kv2.1 inhibition not only in DRG tissue but also other tissues including sciatic nerve and spinal cord, although we focused on DRG tissue research in the current work.

According to the published reports, *db*/*db* mice exhibited DPN symptoms (in presence of hyperalgesia) at early stage [71–73]. It was interesting to find that SP6616 exhibited no beneficial effects on the DPN-like pathology of *db*/*db* mice aged 7-11 week with hyperalgesia (Fig. S9a-c; tactile allodynia, thermal sensitivity and MNCV), although it effectively improved the DPN-like pathology of *db*/*db* mice at late stage (aged 18-22 week) with hypoalgesia. Thus, our results have revealed the potential of SP6616 in preventing the occurrence of diabetic foot.

Given that Kv2.1 channel is expressed in many tissues including renal, hepatic, cardiac, islets β cells and brain, we also inspected the classical markers of renal (creatinine, urea nitrogen), hepatic (ALT, AST) and cardiac function (cardiac troponin-T, cardiac troponin-I) in the serum of mice trying to evaluate the preliminary safety of SP6616. Our results (Fig. S10 a-l) indicated that administration of SP6616 rendered no obviously pharmacological toxicities on mice, although much work needs to be addressed such as structure-activity relationship study, toxicology research and pharmacokinetics assay.

In conclusion, as summarized in the proposed schematic diagram (Fig. 8k), small molecular compound SP6616 as a selective Kv2.1 inhibitor efficiently ameliorated DPN-like pathology of diabetic mice. It improved mitochondrial dysfunction through Kv2.1/CaMKKβ/AMPK/PGC-1α pathway, suppressed inflammation by inhibiting Kv2.1/NF-κB signaling and alleviated apoptosis of DRG neuron through Kv2.1-mediated regulation of Bcl-2 family proteins and Caspase-3 in diabetic mice.

Funding source

This work was supported by National Science & Technology Major Project “Key New Drug Creation and Manufacturing Program”, China (Number:2018ZX09711002), the National Natural Science Foundation for Young Scientists of China (81703806), Postgraduate Research & Practice Innovation Program of Jiangsu Province (KYCX18_1600), the Open Project Program of Jiangsu Key Laboratory for Pharmacology and Safety Evaluation of Chinese Materia Medica (No. JKLPSE201801), the Project of the Priority Academic Program Development of Jiangsu Higher Education Institutions (PAPD), Priority Academic Program Development of Jiangsu Higher Education Institutions (Integration of Chinese and Western Medicine) and Innovative Talent Team of Six Talent Peaks Project in Jiangsu Province (TD-SWYY-013).The funders had no roles in study design, data collection, data analysis, interpretation, writing of the report.

Declaration of Competing Interest

The authors declare no conflicts of interest.

Acknowledgments

The authors thank Xue Lu for technical support.

Supplementary materials

Supplementary material associated with this article can be found, in the online version, at doi:10.1016/j.ebiom.2020.103061.

References

[1] Liu XS, Fan B, Szalad A, Jia L, Wang L, Wang X, et al. MicroRNA-146a mimics reduce the peripheral neuropathy in type 2 diabetic mice. Diabetes 2017;66(12):3111–21.
[2] Bansal D, Badhan Y, Gudala K, Schifano F. Ruboxistaurin for the treatment of diabetic peripheral neuropathy: a systematic review of randomized clinical trials. Diabetes Metab J 2013;37(5):375–84.
[3] Calcutt NA, Smith DR, Frizzi K, Sabbir MG, Chowdhury SK, Mixcoatl-Zecuatl T, et al. Selective antagonism of muscarinic receptors is neuroprotective in peripheral neuropathy. J Clin Invest 2017;127(2):608–22.
[4] Brooks B, Delaney-Robinson C, Molyneaux L, Yue DK. Endothelial and neural regulation of skin microvascular blood flow in patients with diabetic peripheral neuropathy: effect of treatment with the isoform-specific protein kinase C beta inhibitor, ruboxistaurin. J Diabetes Compl 2008;22(2):88–95.
[5] Roman-Pintos LM, Villegas-Rivera G, Rodriguez-Carrizalez AD, Miranda-Diaz AG, Cardona-Munoz EG. Diabetic polyneuropathy in type 2 diabetes mellitus: inflammation, oxidative stress, and mitochondrial function. J Diabetes Res 2016;2016:1–16.
[6] Rojas DR, Kuner R, Agarwal N. Metabolomic signature of type 1 diabetes-induced sensory loss and nerve damage in diabetic neuropathy. J Mol Med (Berl) 2019;97(6):845–54.

[7] Prabodha LBL, Sirisena ND, Dissanayake VHW. Susceptible and prognostic genetic factors associated with diabetic peripheral neuropathy: a comprehensive literature review. Int J Endocrinol 2018;2018:1–9.
[8] Hosseini A, Abdollahi M. Diabetic neuropathy and oxidative stress: therapeutic perspectives. Oxid Med Cell Longev 2013;2013:1–15.
[9] Singh R, Kishore L, Kaur N. Diabetic peripheral neuropathy: current perspective and future directions. Pharmacol Res 2014;80:21–35.
[10] Yang CT, Lu GL, Hsu SF, MacDonald I, Chiou LC, Hung SY, et al. Paeonol promotes hippocampal synaptic transmission: The role of the Kv2.1 potassium channel. Eur J Pharmacol 2018;827:227–37.
[11] Wei Y, Shin MR, Sesti F. Oxidation of KCNB1 channels in the human brain and in mouse model of Alzheimer's disease. Cell Death Dis 2018;9(8):820.
[12] Li H, Shin SE, Seo MS, An JR, Choi IW, Jung WK, et al. The anti-diabetic drug dapagliflozin induces vasodilation via activation of PKG and Kv channels. Life Sci 2018;197:46–55.
[13] Regnier G, Bocksteins E, Van de Vijver G, Snyders DJ, van Bogaert PP. The contribution of Kv2.2-mediated currents decreases during the postnatal development of mouse dorsal root ganglion neurons. Physiol Rep 2016;4(6):1–13.
[14] Jukkola PI, Lovett-Racke AE, Zamvil SS, Gu C. K^+ channel alterations in the progression of experimental autoimmune encephalomyelitis. Neurobiol Dis 2012;47(2):280–93.
[15] Busserolles J, Tsantoulas C, Eschalier A, Lopez Garcia JA. Potassium channels in neuropathic pain: advances, challenges, and emerging ideas. Pain 2016;157(Suppl 1):S7–14.
[16] Chen X, Luo Z, Yang H, Huang Y, Xie S. Examination of a demyelinated fiber by action-potential-encoded second harmonic generation2012;8216:1-8.
[17] Berret E, Kim SE, Lee SY, Kushmerick C, Kim JH. Functional and structural properties of ion channels at the nerve terminal depends on compact myelin. J Physiol 2016;594(19):5593–609.
[18] Boiko N, Kucher V, Eaton BA, Stockand JD. Inhibition of neuronal degenerin/epithelial Na+ channels by the multiple sclerosis drug 4-aminopyridine. J Biol Chem 2013;288(13):9418–27.
[19] Chowdhury SK, Smith DR, Fernyhough P. The role of aberrant mitochondrial bioenergetics in diabetic neuropathy. Neurobiol Dis 2013;51:56–65.
[20] Roy Chowdhury SK, Smith DR, Saleh A, Schapansky J, Marquez A, Gomes S, et al. Impaired adenosine monophosphate-activated protein kinase signalling in dorsal root ganglia neurons is linked to mitochondrial dysfunction and peripheral neuropathy in diabetes. Brain 2012;135(Pt 6):1751–66.
[21] Wang P, Jiang Y, Wang Y, Shyy JY, DeFea KA. Beta-arrestin inhibits CAMKKbeta-dependent AMPK activation downstream of protease-activated-receptor-2. BMC Biochem 2010;11:1–14.
[22] Yang SN, Shi Y, Yang G, Li Y, Yu J, Berggren PO. Ionic mechanisms in pancreatic beta cell signaling. Cell Mol Life Sci 2014;71(21):4149–77.
[23] Firth AL, Gordienko DV, Yuill KH, Smirnov SV. Cellular localization of mitochondria contributes to Kv channel-mediated regulation of cellular excitability in pulmonary but not mesenteric circulation. Am J Physiol Lung Cell Mol Physiol 2009;296(3):L347–60.
[24] Luo Q, Feng Y, Xie Y, Shao Y, Wu M, Deng X, et al. Nanoparticle-microRNA-146a-5p polyplexes ameliorate diabetic peripheral neuropathy by modulating inflammation and apoptosis. Nanomedicine 2019;17:188–97.
[25] Shepherd AJ, Loo L, Gupte RP, Mickle AD, Mohapatra DP. Distinct modifications in Kv2.1 channel via chemokine receptor CXCR4 regulate neuronal survival-death dynamics. J Neurosci 2012;32(49):17725–39.
[26] Zhou TT, Quan LL, Chen LP, Du T, Sun KX, Zhang JC, et al. SP6616 as a new Kv2.1 channel inhibitor efficiently promotes beta-cell survival involving both PKC/Erk1/2 and CaM/PI3K/Akt signaling pathways. Cell Death Dis 2016;7:e2216.
[27] Saleh A, Roy Chowdhury SK, Smith DR, Balakrishnan S, Tessler L, Martens C, et al. Ciliary neurotrophic factor activates NF-kappaB to enhance mitochondrial bioenergetics and prevent neuropathy in sensory neurons of streptozotocin-induced diabetic rodents. Neuropharmacology 2013;65:65–73.
[28] Zhang QP, Zhang HY, Zhang XF, Zhao JH, Ma ZJ, Zhao D, et al. srGAP3 promotes neurite outgrowth of dorsal root ganglion neurons by inactivating RAC1. Asian Pac J Trop Med 2014;7(8):630–8.
[29] Fan B, Li C, Szalad A, Wang L, Pan W, Zhang R, et al. Mesenchymal stromal cell-derived exosomes ameliorate peripheral neuropathy in a mouse model of diabetes. Diabetologia 2020;63(2):431–43.
[30] Reda HM, Zaitone SA, Moustafa YM. Effect of levetiracetam versus gabapentin on peripheral neuropathy and sciatic degeneration in streptozotocin-diabetic mice: Influence on spinal microglia and astrocytes. Eur J Pharmacol 2016;771:162–72.
[31] Watcho P, Stavniichuk R, Tane P, Shevalye H, Maksimchyk Y, Pacher P, et al. Evaluation of PMI-5011, an ethanolic extract of Artemisia dracunculus L., on peripheral neuropathy in streptozotocin-diabetic mice. Int J Mol Med 2011;27(3):299–307.
[32] Obrosova IG, Ilnytska O, Lyzogubov VV, Pavlov IA, Mashtalir N, Nadler JL, et al. High-fat diet induced neuropathy of pre-diabetes and obesity: effects of "healthy" diet and aldose reductase inhibition. Diabetes 2007;56(10):2598–608.
[33] Miranda HF, Sierralta F, Jorquera V, Poblete P, Prieto JC, Noriega V. Antinociceptive interaction of gabapentin with minocycline in murine diabetic neuropathy. Inflammopharmacology 2017;25(1):91–7.
[34] Muller KA, Ryals JM, Feldman EL, Wright DE. Abnormal muscle spindle innervation and large-fiber neuropathy in diabetic mice. Diabetes 2008;57(6):1693–701.
[35] De Gregorio C, Contador D, Campero M, Ezquer M, Ezquer F. Characterization of diabetic neuropathy progression in a mouse model of type 2 diabetes mellitus. Biol Open 2018;7(9):1–9.
[36] Leiter EH, Coleman DL, Ingram DK, Reynolds MA. Influence of dietary carbohydrate on the induction of diabetes in C57BL/KsJ-db/db diabetes mice. J Nutr 1983;113(1):184–95.
[37] Li XN, Herrington J, Petrov A, Ge L, Eiermann G, Xiong Y, et al. The role of voltage-gated potassium channels Kv2.1 and Kv2.2 in the regulation of insulin and somatostatin release from pancreatic islets. J Pharmacol Exp Ther 2013;344(2):407–16.
[38] Jacobson DA, Kuznetsov A, Lopez JP, Kash S, Ammala CE, Philipson LH. Kv2.1 ablation alters glucose-induced islet electrical activity, enhancing insulin secretion. Cell Metab 2007;6(3):229–35.
[39] Rauch JN, Luna G, Guzman E, Audouard M, Challis C, Sibih YE, et al. LRP1 is a master regulator of tau uptake and spread. Nature 2020;580(7803):381–5.
[40] Ohoka N, Okuhira K, Ito M, Nagai K, Shibata N, Hattori T, et al. In vivo knockdown of pathogenic proteins via S pecific and N ongenetic I nhibitor of apoptosis protein (IAP)-dependent P rotein Er asers (SNIPERs). J Biol Chem 2017;292:4556–70.
[41] Sureban SM, May R, George RJ, Dieckgraefe BK, Mcleod HL, Ramalingam S, et al. Knockdown of RNA binding protein musashi-1 leads to tumor regression in vivo. Gastroenterology 2008;134(5):1448–58.
[42] Drude S, Geissler A, Olfe J, Starke A, Domanska G, Schuett C, et al. Side effects of control treatment can conceal experimental data when studying stress responses to injection and psychological stress in mice. Lab Anim (NY) 2011;40(4):119–28.
[43] Armario A, Escorihuela RM, Nadal R. Long-term neuroendocrine and behavioural effects of a single exposure to stress in adult animals. Neurosci Biobehav Rev 2008;32(6):1121–35.
[44] Besch EL, Chou BJ, Cornelius CE. Physiological responses to blood collection methods in rats. Proc Soc Exp Biol Med 1971;138(3):1019–21.
[45] Pesaresi M, Giatti S, Spezzano R, Romano S, Diviccaro S, Borsello T, et al. Axonal transport in a peripheral diabetic neuropathy model: sex-dimorphic features. Biol Sex Differ 2018;9(1):1–14.
[46] Urban MJ, Pan P, Farmer KL, Zhao H, Blagg BS, Dobrowsky RT. Modulating molecular chaperones improves sensory fiber recovery and mitochondrial function in diabetic peripheral neuropathy. Exp Neurol 2012;235(1):388–96.
[47] Kan HW, Hsieh JH, Chien HF, Lin YH, Yeh TY, Chao CC, et al. CD40-mediated HIF-1alpha expression underlying microangiopathy in diabetic nerve pathology. Dis Model Mech 2018;11(4):1–12.
[48] Jacobson DA, Mendez F, Thompson M, Torres J, Cochet O, Philipson LH. Calcium-activated and voltage-gated potassium channels of the pancreatic islet impart distinct and complementary roles during secretagogue induced electrical responses. J Physiol 2010;588(Pt 18):3525–37.
[49] Yang XW, Liu FQ, Guo JJ, Yao WJ, Li QQ, Liu TH, et al. Antioxidation and anti-inflammatory activity of Tang Bi Kang in rats with diabetic peripheral neuropathy. BMC Complement Altern Med 2015;15:66.
[50] Noack M, Kolopp-Sarda M-N. Cytokines et inflammation: physiologie, physiopathologie et utilisation thérapeutique. Revue Francophone des Laboratoires 2018;2018(499):28–37.
[51] Mora E, Guglielmotti A, Biondi G, Sassone-Corsi P. Bindarit: an anti-inflammatory small molecule that modulates the NFkappaB pathway. Cell Cycle 2012;11(1):159–69.
[52] Xing D, Oparil S, Yu H, Gong K, Feng W, Black J, et al. Estrogen modulates NFkappaB signaling by enhancing IkappaBalpha levels and blocking p65 binding at the promoters of inflammatory genes via estrogen receptor-beta. PLoS One 2012;7(6):e36890.
[53] Justice JA, Schulien AJ, He K, Hartnett KA, Aizenman E, Shah NH. Disruption of KV2.1 somato-dendritic clusters prevents the apoptogenic increase of potassium currents. Neuroscience 2017;354:158–67.
[54] Yoon MK, Kim BY, Lee JY, Ha JH, Kim SA, Lee DH, et al. Cytoplasmic pro-apoptotic function of the tumor suppressor p73 is mediated through a modified mode of recognition of the anti-apoptotic regulator Bcl-XL. J Biol Chem 2018;293(51):19546–58.
[55] Venkatesan RS, Sadiq AM. Effect of morin-5′-sulfonic acid sodium salt on the expression of apoptosis related proteins caspase 3, Bax and Bcl 2 due to the mercury induced oxidative stress in albino rats. Biomed Pharmacother 2017;85:202–8.
[56] Fan J, Zhang N, Yin G, Zhang Z, Cheng G, Qian W, et al. Edaravone protects cortical neurons from apoptosis by inhibiting the translocation of BAX and Increasing the interaction between 14-3-3 and p-BAD. Int J Neurosci 2012;122(11):665–74.
[57] Siow NL, Xie HQ, Choi RC, Tsim KW. ATP induces the post-synaptic gene expression in neuron-neuron synapses: Transcriptional regulation of AChE catalytic subunit. Chem Biol Interact 2005;157-158:423–6.
[58] Gilon P, Chae HY, Rutter GA, Ravier MA. Calcium signaling in pancreatic beta-cells in health and in Type 2 diabetes. Cell Calcium 2014;56(5):340–61.
[59] Messinger RB, Naik AK, Jagodic MM, Nelson MT, Lee WY, Choe WJ, et al. In vivo silencing of the Ca(V)3.2 T-type calcium channels in sensory neurons alleviates hyperalgesia in rats with streptozocin-induced diabetic neuropathy. Pain 2009;145(1-2):184–95.
[60] Chung YC, Lim JH, Oh HM, Kim HW, Kim MY, Kim EN, et al. Calcimimetic restores diabetic peripheral neuropathy by ameliorating apoptosis and improving autophagy. Cell Death Dis 2018;9(12):1163.
[61] Li J, Hu X, Liang F, Liu J, Zhou H, Liu J, et al. Therapeutic effects of moxibustion simultaneously targeting Nrf2 and NF-kappaB in diabetic peripheral neuropathy. Appl Biochem Biotechnol 2019;189(4):1167–82.
[62] Yao W, Yang X, Zhu J, Gao B, Shi H, Xu L. IRE1alpha siRNA relieves endoplasmic reticulum stress-induced apoptosis and alleviates diabetic peripheral neuropathy in vivo and in vitro. Sci Rep 2018;8(1):2579.
[63] Stirban A. Microvascular dysfunction in the context of diabetic neuropathy. Curr Diab Rep 2014;14(11):541.
[64] Begandt D, Good ME, Keller AS, DeLalio LJ, Rowley C, Isakson BE, et al. Pannexin channel and connexin hemichannel expression in vascular function and inflammation. BMC Cell Biol 2017;18(Suppl 1):2.
[65] Huang Y, Hu B, Zhu J. Study on the use of quantitative ultrasound evaluation of diabetic neuropathy in the rat sciatic nerve. Australas Phys Eng Sci Med 2016;39(4):997–1005.

[66] Tang W, Chen X, Liu H, Lv Q, Zou J, Shi Y, et al. Expression of Nrf2 promotes schwann cell-mediated sciatic nerve recovery in diabetic peripheral neuropathy. Cell Physiol Biochem 2018;46(5):1879–94.
[67] Yorek MA. Vascular impairment of epineurial arterioles of the sciatic nerve: implications for diabetic peripheral neuropathy. Rev Diabet Stud 2015;12(1-2):13–28.
[68] Selvarajah D, Wilkinson ID, Emery CJ, Harris ND, Shaw PJ, Witte DR, et al. Early involvement of the spinal cord in diabetic peripheral neuropathy. Diabetes Care 2006;29(12):2664–9.
[69] Jia Y, Shen Z, Lin G, Nie T, Zhang T, Wu R. Lumbar spinal cord activity and blood biochemical changes in individuals with diabetic peripheral neuropathy during electrical stimulation. Front Neurol 2019;10:222.
[70] Jolivalt CG, Lee CA, Ramos KM, Calcutt NA. Allodynia and hyperalgesia in diabetic rats are mediated by GABA and depletion of spinal potassium-chloride co-transporters. Pain 2008;140(1):48–57.
[71] Jia L, Chopp M, Wang L, Lu X, Szalad A, Zhang ZG. Exosomes derived from high-glucose-stimulated Schwann cells promote development of diabetic peripheral neuropathy. The FASEB J 2018;32(12):6911–22.
[72] Cheng HT, Dauch JR, Hayes JM, Hong Y, Feldman EL. Nerve growth factor mediates mechanical allodynia in a mouse model of type 2 diabetes. J Neuropathol Exp Neurol 2009;68(11):1229–43.
[73] Xu X, Chen H, Ling BY, Xu L, Cao H, Zhang YQ. Extracellular signal-regulated protein kinase activation in spinal cord contributes to pain hypersensitivity in a mouse model of type 2 diabetes. Neurosci Bull 2014;30(1):53–66.